INVESTIGATION OF SURFACE-JET THERMAL OUTFALL FOR IATAN STEAM ELECTRIC GENERATING STATION

by

William W. Sayre

Prepared for
Black and Veatch Consulting Engineers
Kansas City, Missouri

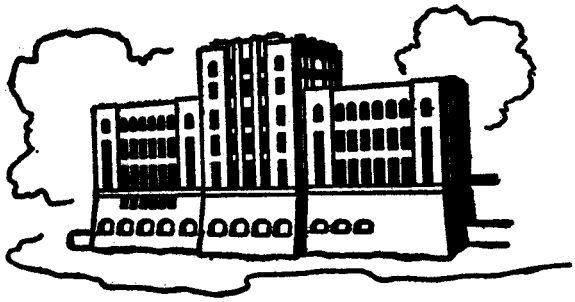

IIHR Report No. 167

Iowa Institute of Hydraulic Research
The University of Iowa
Iowa City, Iowa

April 1975

INVESTIGATION OF SURFACE-JET THERMAL OUTFALL FOR IATAN STEAM ELECTRIC GENERATING STATION

by

William W. Sayre

Prepared for
Black and Veatch Consulting Engineers
Kansas City, Missouri

IIHR Report No. 167

Iowa Institute of Hydraulic Research
The University of Iowa
Iowa City, Iowa

April 1975

ABSTRACT

The feasibility of a surface-jet thermal outfall for discharging the condenser cooling water from the proposed Iatan Steam Electric Generating Station into the Missouri River is investigated. Hydrographic measurements by the U. S. Geological Survey show that the geometry of and distribution of flow in the river channel is favorable for a surface-jet scheme.

Downstream temperature-rise distributions are predicted for surface jets discharging both at right angles and parallel to the ambient flow for selected river discharges. The prediction technique takes into account the properties of the ambient flow, including the mixing mechanisms, as well as those of the jet. The right-angle discharge is predicted to be superior in almost every respect. For one-unit operation at full plant load and a river discharge of 10,000 cfs, it is predicted that the 5°F temperature-rise isotherm would cover a horizontal area of less than 0.5 acres and the zone-of-passage wherein the temperature rise is less than 5°F exceeds 85 percent of the river flow.

ACKNOWLEDGMENTS

This investigation was sponsored by Black and Veatch, Consulting Engineers, Kansas City, Missouri, on behalf of the Kansas City Power & Light Company and the St. Joseph Light & Power Company. Messrs. George R. Savage and Herbert R. Temme of Black and Veatch were instrumental in providing much of the background data. Hydrographic surveys in the vicinity of the Iatan Station were performed on February 20, 1974 by U. S. Geological Survey personnel from the Water Resources Division, Iowa District, under the direction of Mr. Ivan L. Burmeister. Mr. Ogbazghi Sium of the Iowa Institute of Hydraulic Research assisted the writer in the computations. Helpful suggestions and criticisms were provided by Profs. Jean-Claude Tatinclaux and John F. Kennedy, also of the Iowa Institute of Hydraulic Research.

TABLE OF CONTENTS

LIST OF TABLES

LIST OF FIGURES

LIST OF FIGURES (continued)

LIST OF SYMBOLS

b_o	Initial jet width in feet
D, D_A, D_J	Diffusion factor in ft^{-1}. Subscripts A & J denote components due to ambient and jet mixing mechanisms respectively
$d, \bar{d}$	Local and width-averaged depth in feet
E_Z, E_{ZA}, E_{ZJ}	Transverse diffusion coeffient in ft^2/sec. Second subscripts. A & J denote components due to ambient and jet mixing mechanisms respectively
$\mathbb{F}_{DA}$	Densimetric Froude number for ambient flow = $\bar{U}_A \Big/ \sqrt{g \frac{\Delta\rho}{\rho} \bar{d}}$
$\mathbb{F}_{DO}$	Initial jet densimetric Froude number = $U_o \Big/ \sqrt{g \frac{\Delta\rho}{\rho} h_o}$
g	Acceleration of gravity = 32.2 ft/sec^2
h_o	Initial jet height in feet
i	Subscript denoting subreach number
p	Dimensionless cumulative discharge per unit width = q_c/Q_R or $\Delta q_c/Q_R$, measured from peak of transverse temperature-rise distribution curve
Q_o	Jet discharge in ft^3/sec (cfs)
Q_R	Ambient river discharge in ft^3/sec (cfs)
$q, \bar{q}$	Local and width-averaged discharge per unit width in ft^2/sec
q_c	Cumulative discharge measured from Missouri shore, in ft^3/sec (cfs)
q_{cp}	Cumulative discharge at plume centerline, in ft^3/sec (cfs)
Δq_c	Incremental cumulative discharge measured from plume centerline = $q_c - q_{cp}$ in ft^3/sec (cfs)
$\Delta q_{cl/2}$	Incremental cumulative discharge measured from plume centerline, in either direction, within which $\Delta T \geq \Delta T_p/2$, in ft^3/sec (cfs)
q_{zp}	Discharge per unit width in portion of channel occupied by plume, in ft^2/sec
R	Ratio of initial jet velocity to average ambient velocity = $U_o/\bar{U}_A$

LIST OF SYMBOLS (continued)

r_c	Radius of curvature of bend in feet
ΔT	Temperature rise above ambient temperature in °F or °C
ΔT_o	Initial temperature rise of jet at outfall in °F or °C
ΔT_p	Maximum temperature rise in cross section in °F or °C
$\bar{U}_A$	Average velocity of ambient flow in ft/sec
U_o	Initial jet velocity in ft/sec
$\bar{u}^d$	Depth-averaged local velocity of flow in ft/sec
U_*	Shear velocity of mean ambient flow = $\sqrt{g\bar{d}S}$, where S = longitudinal channel slope, in ft/sec
W	Width of channel at water surface in feet
x	Distance downstream from outfall in feet
x_i	Longitudinal coordinate distance at downstream end of i'th subreach, in feet
x_{oi}	Longitudinal coordinate distance at location of virtual source for i'th subreach, in feet
z	Transverse distance measured from Missouri shore, in ft
Δz	Incremental transverse distance measured from plume centerline, in feet
α	Angle between plume centerline and direction of ambient flow, in degrees
ζ	Dimensionless incremental discharge per unit width measured from plume centerline = $\Delta q_c/Q_o(\xi/\xi_o)^{\frac{1}{2}}$ = $(\Delta q_c/Q_R)/2\sqrt{\pi D\xi}$
θ	Dimensionless temperature rise = $\Delta T/\Delta T_o$
ξ	Downstream distance from outfall measured along plume centerline, in feet
ξ_o	Length of zone of flow establishment for jet, measured along plume centerline, in feet
$\Delta\rho/\rho$	Ratio of density difference between ambient and heated water to density of ambient water

INVESTIGATION OF SURFACE-JET THERMAL OUTFALL FOR IATAN STEAM ELECTRIC GENERATING STATION

I. BACKGROUND

At the request of Black and Veatch, Consulting Engineers, the Iowa Institute of Hydraulic Research undertook an investigation to predict the performance of a surface-jet thermal outfall for discharging the condenser cooling water from the proposed Iatan Steam Electric Generating Station into the Missouri River. Located near Iatan, Missouri, at about Mile 411 on the Missouri River, the Iatan Station will be a major coal-fired facility that is operated jointly by Kansas City Power & Light Company and St. Joseph Light & Power Company. Present planning calls for the eventual installation of a total generating capacity of about 3,000 megawatts, made up of four units. Units 1 and 2 will be rated at 630 megawatts each, and units 3 and 4 at about 900 megawatts each. Units 1 and 2 are tentatively scheduled to go into commercial operation in April 1979 and April 1981, respectively. Dates have not been established as yet for the construction and operation of units 3 and 4.

Units 1 and 2 will each require a combined condenser and auxiliary cooling water flow of 746 cubic feet per second (cfs) which will be withdrawn from the river, pumped through the circulatory water system, and returned to the river through an outfall structure. The temperature rises in the condenser flow are 10.7°F, 14.2°F, and 18.7°F, corresponding to average, maximum and peak turbine operating conditions. The peak rise of 18.7°F is used in the calculations presented later in this report.

This report describes first the hydraulic and hydrologic characteristics of the Missouri River in the vicinity of the Iatan Station, with a view toward determining the hydraulic conditions in the river channel over a range of low to medium river flows wherein the performance of a single-point, surface-jet outfall system is least likely to be satisfactory. For these flow conditions, the location and areal extent of the 10°F, 5°F and 1°C temperature rise isotherms are predicted for one-unit operation at peak load. Transverse dis-

tributions of depth-averaged temperature rise are also predicted for several selected cross section.

Federal and State standards governing the discharge of thermal effluents into the Missouri River between Missouri and Kansas are still in a state of flux. At present, the excess temperature in the river due to a thermal discharge is not to exceed $5^{\circ}F$ outside of an initial mixing zone. Aside from the guideline that the mixing zone should not occupy more than 25 percent of the cross-sectional area of the channel, the size of the mixing zone is not specified. There is also an absolute maximum temperature limitation of $90^{\circ}F$. Temperature records for the period from May 1967 through December 1973 for the intake at the St. Joseph Light & Power Company's generating station exceeded $85^{\circ}F$ on only four days, and then only for periods of less than one day in duration. Therefore the $5^{\circ}F$ excess temperature limitation would almost always be the controlling criterion. Proposed federal standards, if adopted, would permit operation of open-cycle cooling systems for steam electric power generating facilities only in exceptional circumstances.

II. DESCRIPTION OF RIVER IN VICINITY OF IATAN STATION

A. General Description. The site for the Iatan Station is located on the outside of Upper Iatan Bend at about Mile 411 in a gently sinuous reach of the river, as shown on Fig. 1. The channel is constrained by a system of rock-filled revetments, dikes, and jetties to a width of about 500 to 800 feet at bank-full discharge, and an alignment consisting of a series of smooth bends. The channel bottom consists predominantly of fine sand. The channel slope over the reach from Mile 416 to Mile 404 is about 0.00019 (9). During the navigation season, which lasts from April through November, the river discharge is maintained at not less than about 35,000 cfs. During the remaining months, the discharge may drop to considerably lower levels, particularly during ice jams. Depending on discharge and temperature, the configuration of the channel bed may vary widely. In an extensively studied reach near Omaha (10), a configuration consisting of large dunes and bars is typical for the spring and summer months. This generally gives way to a much smoother plane-bed configuration during the fall.

B. Relevant Hydrologic Characteristics. The discharge of the

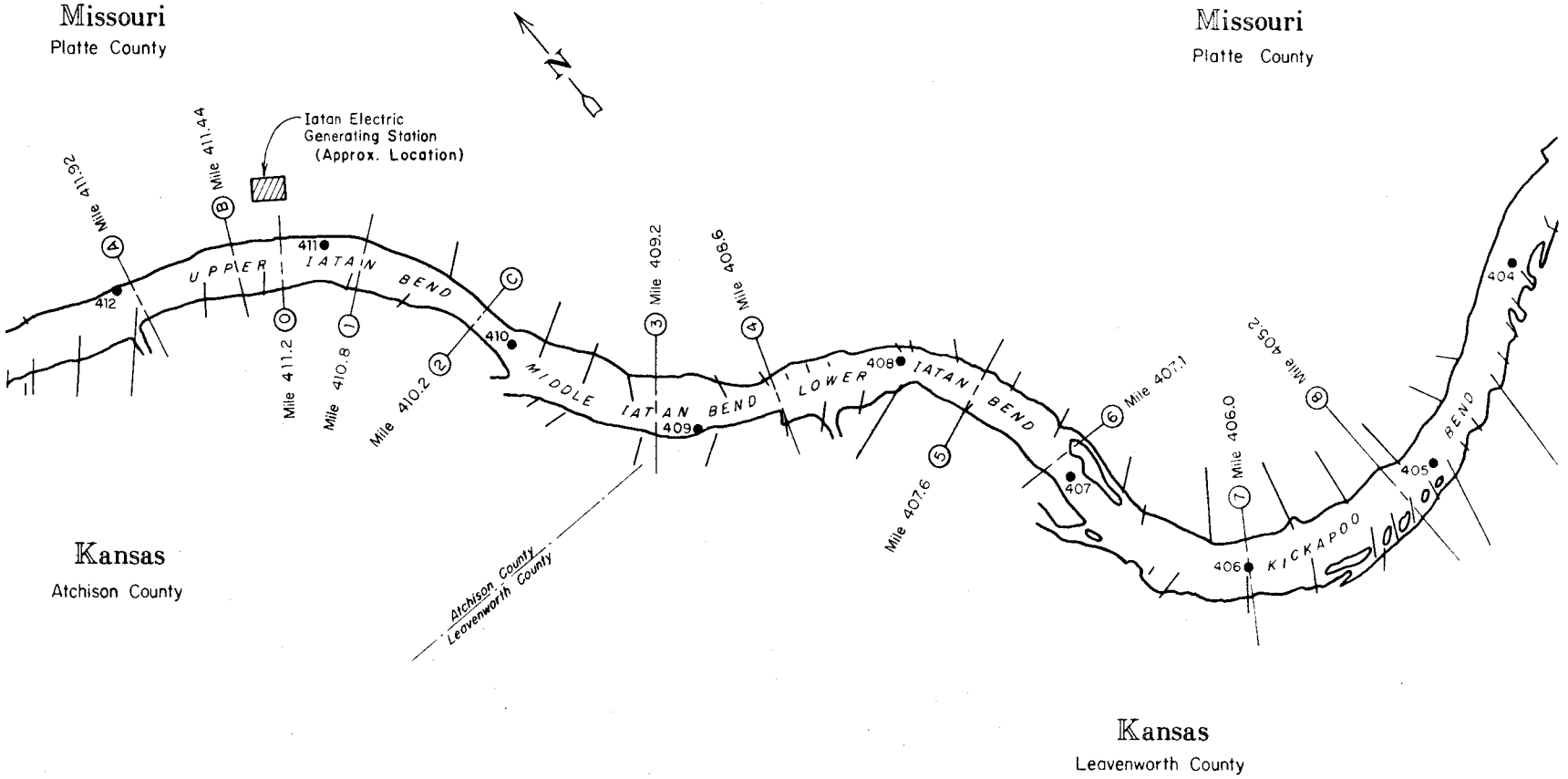

Figure 1. Map of Missouri River near Iatan Station

Missouri River is largely controlled by an extensive system of flood-control, hydro-electric power, and irrigation reservoirs both on the main stream, upstream from Iowa, and on the major tributaries. Since the development of this system, which took place largely between 1930 and 1960, extreme high and low flows have been largely eliminated. Some statistics on low flows are given in Table 1. They are taken from statistical summaries prepared by the Iowa and Missouri District Offices of the Water Resources Division of the U. S. Geological Survey for the USGS gaging stations at Rulo, Nebraska, and St. Joseph, Missouri.

Normally the data for St. Joseph would be more relevant for the Iatan Station because it is only 37 miles upstream from the plant site, whereas Rulo is 87 miles upstream. Also, there may be significant tributary inflow between Rulo and St. Joseph. However, because of the more recent period of observation for Rulo, which began when the river control system was nearing completion, the data for Rulo in Table 1 are considered to be more relevant. Three river discharges, namely 35,000 cfs, 20,000 cfs and 10,000 cfs, were selected for the ambient flow conditions to be considered in the analysis of the thermal discharges. They represent, respectively, a typical summertime flow, a typical wintertime flow, and a representative low flow which is exceeded on all but about seven days in an average year.

C. USGS Hydrographic Measurements. The transverse distribution of flow in three cross sections near the Iatan site was measured by U. S. Geological Survey personnel from the Water Resources Division, Iowa District Office, Iowa City, on February 20, 1974. The locations of the three cross sections, designated as sections A, B, and C are shown on Fig. 1. The measurements were obtained using the moving boat method, in which the depth of flow and the velocity at a point 2.5 ft below the surface are measured and recorded continuously as the boat moves across the river. The transverse position of the boat is recorded intermittently, and corrections for boat velocity are made. Several traverses are made at each cross section, and the results are averaged. The measured velocity 2.5 ft below the surface is multiplied by 0.9 to estimate the depth-averaged velocity.

The results of the USGS hydrographic measurements are shown in Figs. 2a, 2b, and 2c. These figures show the transverse distribution of depth, d, depth-averaged velocity, $\bar{u}^d$, and discharge per unit width, $q = d\bar{u}^d$, at the time of the field measurements. The abscissa, z, is the distance

Table 1. STATISTICAL DATA ON LOW RIVER FLOWS

Gaging Station	Rulo	St. Joseph
River Mile	498	448
Period of Observation	1956-71	1929-67
Discharge in cfs which is exceeded about 75% of the time	22,000	19,000
Discharge in cfs which is exceeded about 95% of the time	12,500	10,000
Discharge in cfs which is exceeded about 99% of the time	7,800	6,000
Low discharge in cfs for a period of 7 days with a recurrence interval of once in 10 years	6,474	4,374

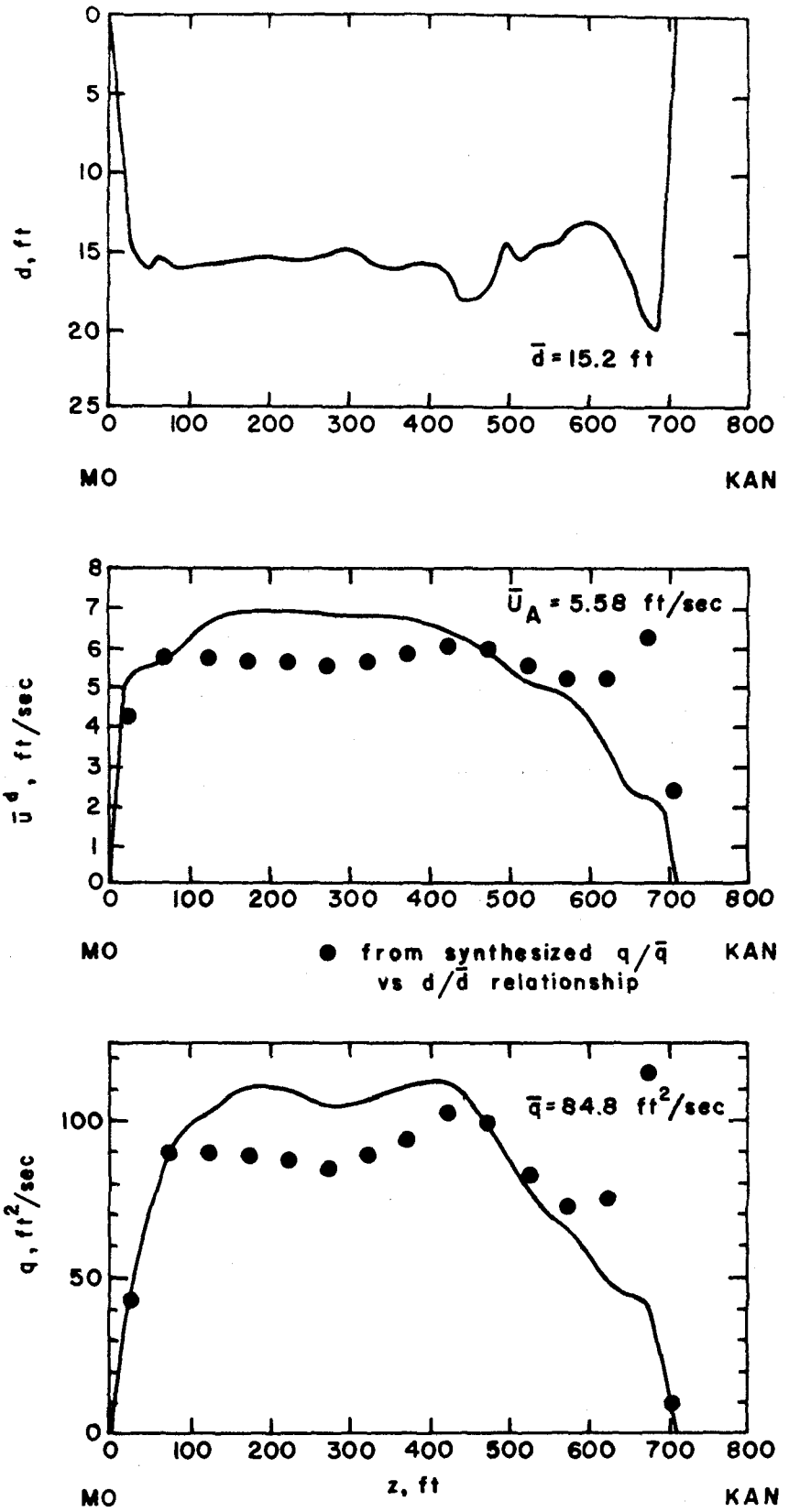

Figure 2a. Transverse distribution of depth, velocity and unit discharge measured by USGS at Mile 411.92.

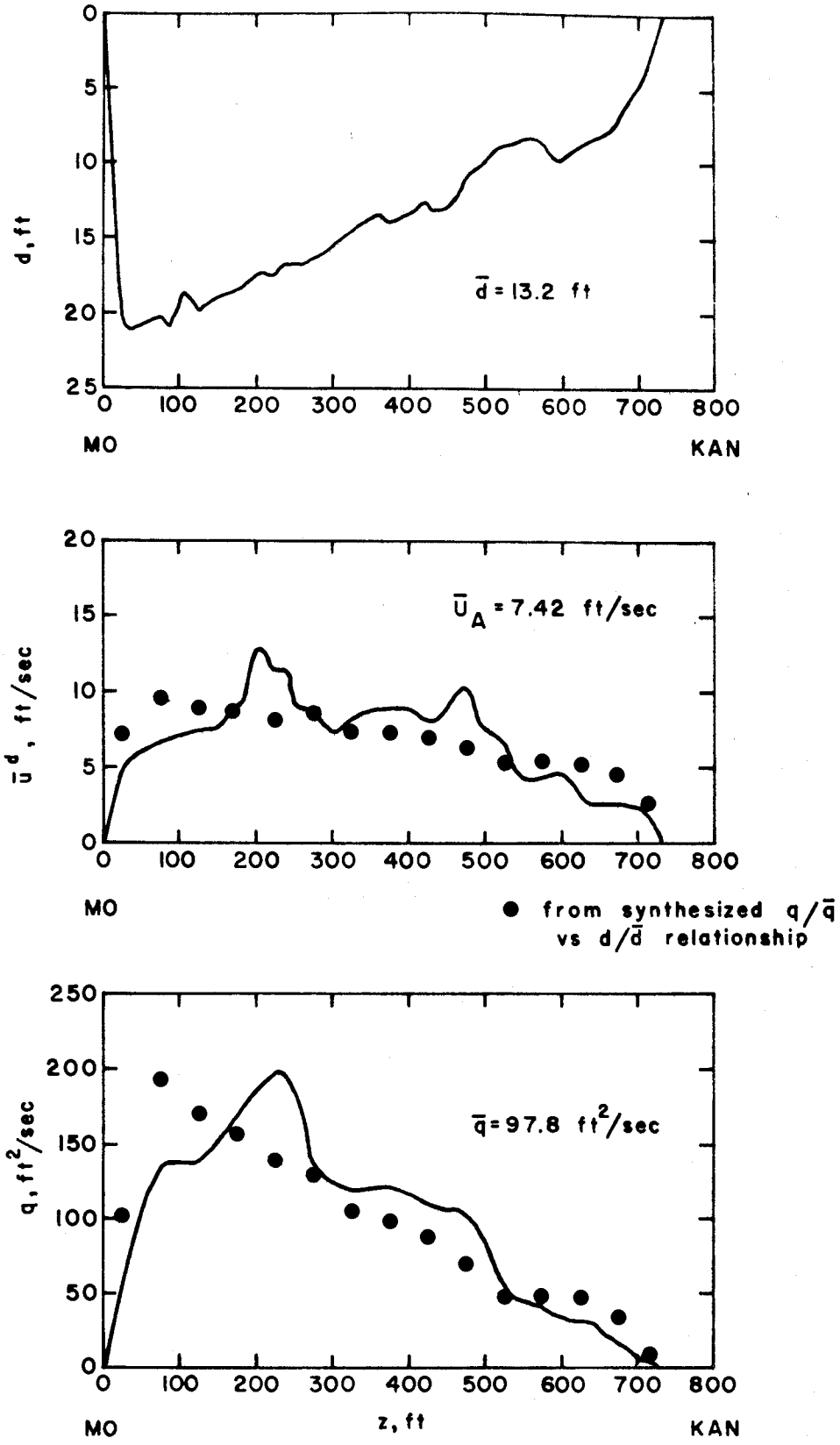

Figure 2b. Transverse distribution of depth, velocity and unit discharge measured by USGS at Mile 411.44.

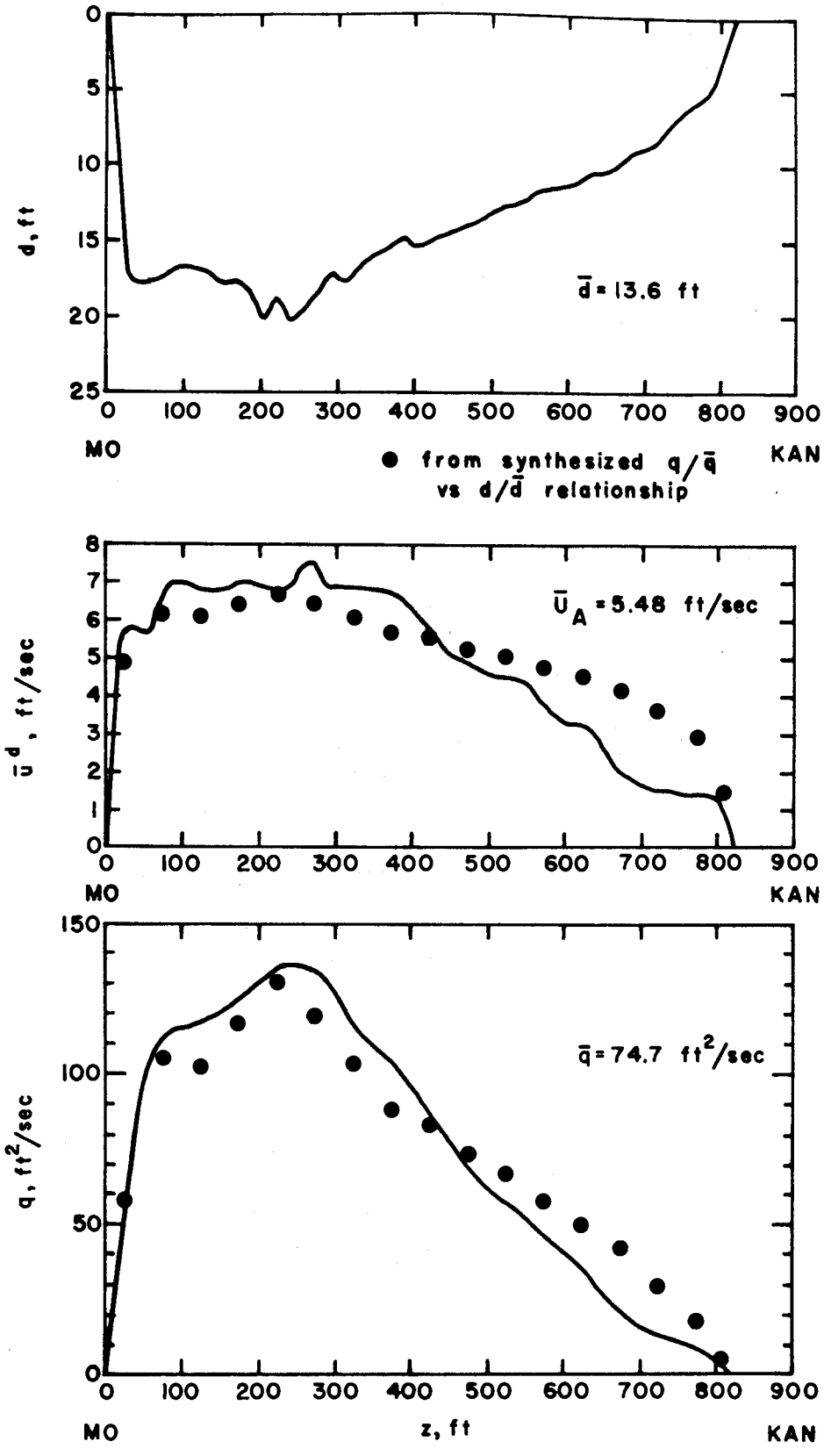

Figure 2c. Transverse distribution of depth, velocity and unit discharge measured by USGS at Mile 410.20.

from the Missouri shore. At section A (Mile 411.92), which is upstream from the plant site, the shape of the cross section is roughly rectangular and the flow is distributed fairly evenly across the channel. At section B (Mile 411.44), near the plant site, and at section C (Mile 410.20) downstream from the plant site, the flow is concentrated toward the Missouri side where the channel is deepest. This is the most favorable kind of flow distribution for a surface jet thermal outfall system because it makes more dilution water available near the point of discharge. Possible variations in the channel shape and discharge distribution are discussed in Part D of this section.

D. Synthesis of Transverse Distribution of Flow at Lower River Discharges. The river discharges determined from the USGS hydrographic measurements for the three sections, from upstream to downstream were 60,200, 71,400, and 61,300 cfs, respectively. The 20 February discharge obtained from the St. Joseph gaging station was 53,400 cfs. For predicting the behavior of the thermal plume at lower river discharges, knowledge of the transverse distribution of the flow at the lower discharges is required. The transverse distributions for the selected lower river discharges, 35,000, 20,000, and 10,000cfs, were estimated using the synthesizing procedure described in the next paragraph.

The synthesizing procedure is based on the hypothesis that a relationship exists between the transverse distributions of the ratios $q/\bar{q}$ and $d/\bar{d}$, where $\bar{q}$ and $\bar{d}$ are, respectively, the width-averaged values of the local discharge per unit width and local depth. Such a relationship could then be used to synthesize the transverse distribution of $q/\bar{q}$ in cross sections for which the distribution of d, but not q, is known.

Figure 3 shows the relationship between $q/\bar{q}$ and $d/\bar{d}$ for the three cross sections where measurements were obtained. The data shown on Fig. 3 were obtained from the distribution curves for d and q given in Figs. 2a, 2b and 2c. The data on Fig. 3 fall fairly close to the relationship

$$\frac{q}{\bar{q}} = \left(\frac{d}{\bar{d}}\right)^{5/3} \qquad (1)$$

which is based on the Manning formula. The writer has compared Eq. 1 with data from elsewhere in the Missouri River (7) and also with data from the Mississippi and Illinois Rivers, and found it to be fairly reliable. As an additional check, synthesized distributions of $\bar{u}^{d}$ and q were computed using Eq. 1 for the three measurement cross sections with the results shown

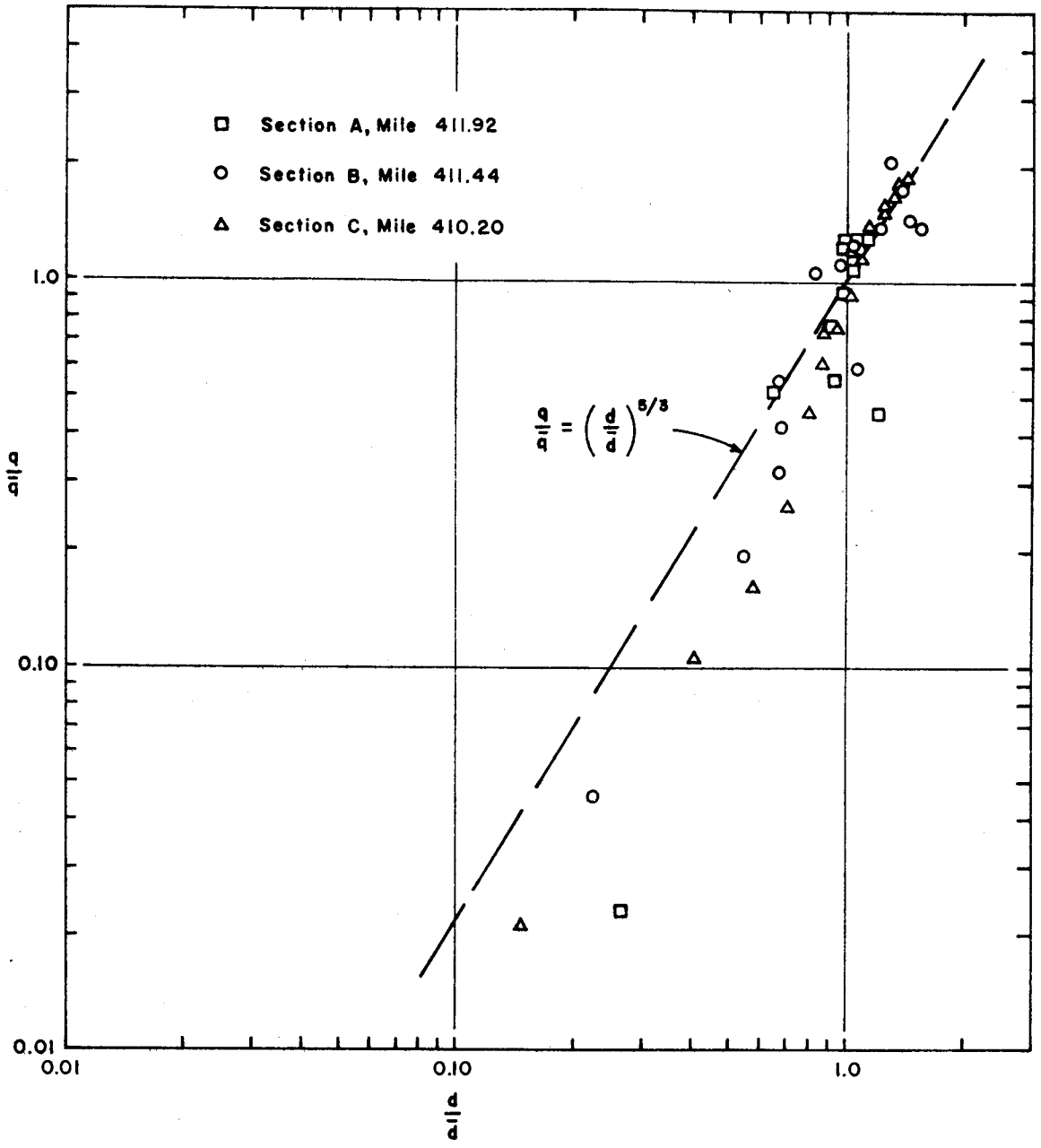

Figure 3. Relative unit discharge versus relative depth relationship for synthesizing transverse distribution of unit discharge.

by the circles plotted on Figs. 2a, 2b and 2c. In order to obtain distributions of q that give the correct total discharge Q, it was necessary to multiply the values of q computed by Eq. 1 by the correction factor Q_m/Q_c, where Q_m is the total measured discharge and Q_c is the total computed discharge for the distribution of q computed by Eq. 1. For the three cross sections, the values of Q_m/Q_c varied from about 0.94 to 0.99.

The transverse flow distributions used in the thermal plume analyses were synthesized from transverse depth-sounding profiles given in the Corps of Engineers November 1972 Hydrographic Survey Sheets (9) for selected cross sections in the Upper, Middle and Lower Iatan Bends and the Kickapoo Bend. The river discharge was 69,000 cfs when these depth soundings were made. Before applying the synthesizing procedure to estimate the transverse distributions of flow in these cross sections for the lower river discharges, it was necessary to determine the drop in water surface elevation corresponding to reductions in discharge. This was done on the basis of an estimated stage versus discharge curve for Mile 411, supplied by Black and Veatch. The resulting drops in water surface elevation corresponding to reductions in river discharge from 69,000 cfs to 35,000 cfs, 20,000 cfs, and 10,000 cfs, are shown in Table 2. To obtain the transverse distribution curves for depth d for the cross sections used in the thermal plume analyses, the water surface levels were dropped by the amounts shown in the last column of Table 2. Distribution curves for $q/\bar{q}$ were then determined using Eq. 1.

In the procedure described above it is implicitly assumed that there is no significant change in the cross sectional shape as the river discharge and depth are reduced, and also that there is a unique stage-discharge relationship. Neither of these assumptions is strictly true for alluvial channels. With regard to the first assumption, there are apt to be different amounts of aggradation and/or degradation of the bed in different parts of the cross section accompanying changes in discharge. With regard to the second assumption, seasonal shifts in the stage-discharge relation may occur that evidently are associated with temperature-related effects on the bed configuration, among other factors. Unfortunately, alluvial channel phenomena are not sufficiently well understood to quantitatively evaluate or significantly improve on the assumptions made above. In the present case, however, the channel shape and transverse flow distribution are certain to retain the general characteristics of larger depths

Table 2. ESTIMATED STAGE VERSUS DISCHARGE AT MILE 411

River Discharge	W. S. Elev. above MSL	Stage	Drop in W.S. Elev. below W.S. Elev. for Q = 69,000 cfs
cfs	ft	ft	ft
69,000	768.7	14.2	---
35,000	763.9	9.4	4.8
20,000	761.0	6.5	7.7
10,000	758.5	4.0	10.2

and discharges per unit width close to the Missouri shore, in the vicinity of the outfall structure.

III. METHODS FOR PREDICTING TEMPERATURE DISTRIBUTIONS

A. General Considerations. Most of the existing methods for predicting the distribution of temperature rises resulting from thermal discharges into aquatic environments are strictly applicable only to large, idealized, water bodies, wherein effects of confining channel boundaries are of secondary importance, and throughout which ambient flow properties are constant. In the case of the discharge from the Iatan station, however, the complicating factors of channel boundaries and varying flow properties are important and must be taken into account.

The only type of outfall structure considered herein is a surface jet entering the river from a fixed rectangular slot. This type of structure is among the most economical. Considering the cross sectional shape of the channel and the transverse flow distribution and relatively high velocity in the channel at the plant site, a single-point outfall at the bank is judged to be feasible for the Iatan Station. Two orientations of the jet are considered: discharge at right angles to the main river flow, and discharge parallel to the main flow.

The basic strategy in the case of the right-angle discharge is to "squirt" the jet far enough out into the main flow so that it mixes with sufficient river water to achieve the required dilution before it is deflected entirely in the downstream direction. The plume trajectory depends on the ratio of the initial cross-channel momentum of the jet to the downstream momentum of the ambient flow. The right-angle jet provides more rapid initial mixing and temperature reduction due to dilution, but it carries further out into the river.

In the case of the parallel discharge, initial mixing is less rapid and the plume would tend to be confined to a narrower zone closer to the shore. However, it must eventually also spread transversely due to the dispersive mechanisms of the ambient flow.

Multiple-point discharge systems, such as submerged diffuser pipes, were not considered in this investigation. Considering that the transverse distrubiton of the ambient flow provides an abundant supply of dilution

water within range of a single-point discharge, the benefits of a multiple-point discharge system would be marginal at best.

B. Modified Carter Relationships for Right-Angle Discharge. Of the various methods that were considered for predicting the behavior of a surface jet discharging normal to an ambient flow, none was found to be entirely satisfactory. A computational method based on the laboratory flume data of Carter, Schiemer and Regier (1) appeared to be the one most nearly applicable to the Iatan Station. Their report includes one set of relationships developed for the case of a three-dimensional jet with minor bottom boundary effects, and another set for the case of a two-dimensional bottom-attached jet. Both sets are applicable in a strict sense only to ambient flows in an idealized rectangular channel. The ranges of values of the various parameters describing the jet and the mean ambient flows in the experiments that were used to verify these relationships included the ranges of interest for the Iatan Station, with one exception. The values of the ratio of jet discharge Q_o to ambient river discharge Q_R are mostly larger for the Iatan Station.

In order to adapt the Carter et al (1) method to the Missouri River, certain modifications were introduced. However, before discussing these, it is helpful to refer to the definition sketch for a jet discharging at right angles into an ambient flow shown in Fig. 4, to fix the variables in mind. The most important modification introduced is the substitution of the normalized cumulative discharge

$$\frac{q_c}{Q_R} = \frac{1}{Q_R} \int_0^z q \, dz \qquad (2)$$

for the normalized transverse distance z/W across the channel. Yotsukura and Cobb (12) have shown that use of q_c rather than z as the primary independent variable permits a simpler mathematical representation of the transverse mixing process in natural channels because it automatically accounts to a considerable extent for variations in flow properties across the channel and for transverse shifts in the ambient flow pattern along the channel. Solutions obtained in the q_c domain can then be transformed to the z domain, if so desired, using Eq. 2 as a mapping function.

The second modification is the introduction of the scaling para-

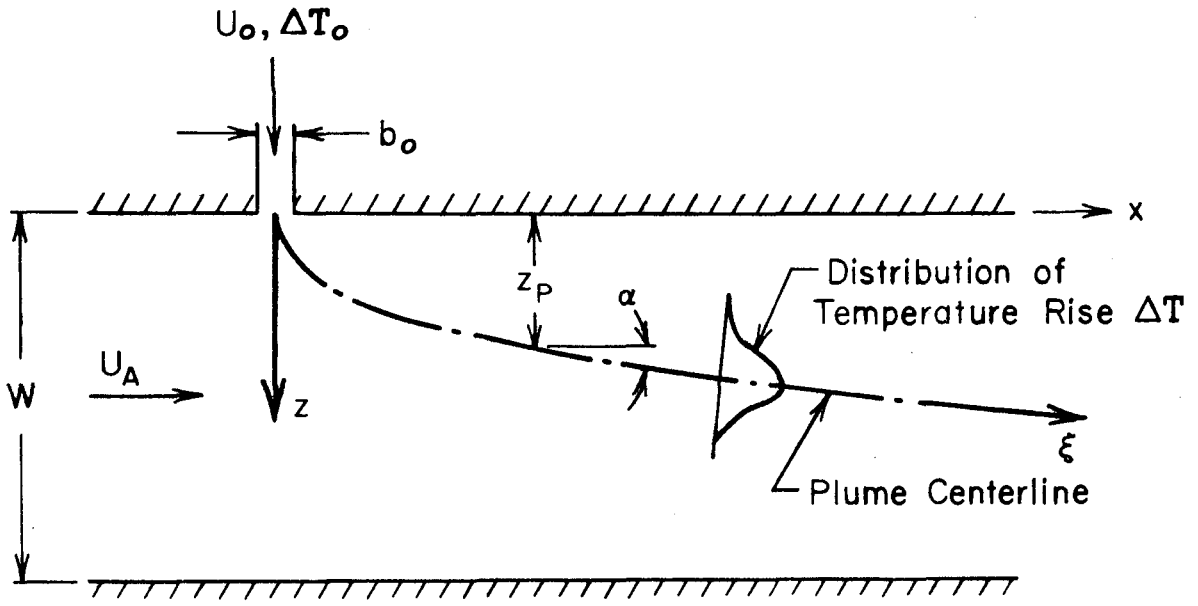

Figure 4. Definition sketch for jet discharging at right angles into ambient flow.

meter

$$\xi_o = 5 \sqrt{b_o h_o} \tag{3}$$

as the length of the zone of flow establishment, measured along the centerline of the plume. In Eq. 3, b_o and h_o are, respectively, the initial jet width and jet height. The corresponding relationships given by Carter et al (1) are

$$\xi_o = 10\, b_o$$

for the two-dimensional jet and

$$\xi_o = 3 \sqrt{b_o h_o}$$

for the three-dimensional jet. Eq. 3 is a compromise between these relationships and corresponding ones based on the data of Stolzenbach and Harleman (8) and of Motz and Benedict (3). It is judged that the thermal discharge at Iatan will behave like a three-dimensional jet initially, but as it expands vertically and encounters the bottom, mixing and entrainment will be retarded and it will begin to behave more like a two-dimensional jet. The transition from three- to two- dimensional behavior should occur sooner as the river discharge and depth decreases.

Finally, the identity based on continuity

$$\frac{Q_o}{Q_R} = \frac{U_o b_o h_o}{\bar{U}_A W \bar{d}} \tag{4}$$

is used as a link between the variables describing the initial properties of the jet and the corresponding mean properties of the ambient flow.

The modified Carter relationships, after incorporating Eqs. 2, 3 and 4, are given by the following equations.

1. Centerline trajectory for two-dimensional jet:

$$\frac{q_{cp}}{Q_R} = A_1 \left(\frac{X}{\xi_o}\right)^{\frac{1}{2}} \tag{5}$$

where

$$A_1 = \sqrt{2\ R\ \frac{Q_o}{Q_R}\ \frac{\bar{d}}{h_o}\ \frac{\xi_o}{W}} \tag{6}$$

q_{cp} = cumulative discharge of ambient flow at the transverse coordinate distance z_p of the plume centerline, and $R = U_o/\bar{U}_A$, the ratio of the initial jet velocity to the mean ambient velocity.

2. Centerline trajectory for three-dimensional jet:

$$\frac{q_{cp}}{Q_R} = A_2 \left(\frac{x}{\xi_o}\right)^{1/3} \tag{7}$$

where

$$A_2 = 0.5372\ \frac{\xi_o}{W}\ R^{2/3} \tag{8}$$

3. Distribution of temperature rise in plume:

$$\frac{\Delta T}{\Delta T_o} = \frac{\Delta T_p}{\Delta T_o}\ \frac{1}{2}\left\{1 + \cos\left(\frac{\pi \Delta q_c}{2\Delta q_{c\frac{1}{2}}}\right)\right\} \tag{9}$$

where

$$\left(\frac{\Delta T_p}{\Delta T_o}\right) = \left(\frac{\xi}{\xi_o}\right)^{-\frac{1}{2}} \tag{10}$$

represents the decay of temperature rise along the plume centerline for a two-dimensional jet, $\Delta q_c = q_c - q_{cp}$, and

$$2\Delta q_{c\frac{1}{2}} = Q_o \left(\frac{\xi}{\xi_o}\right)^{\frac{1}{2}} \tag{11}$$

is the scaling factor for the width of the plume in terms of q_c, defined as the incremental cumulative discharge, measured from the centerline in both directions, within which $\Delta T \geq \Delta T_p/2$.

4. Width of plume within which temperature rise $\geq \Delta T$:

$$\frac{2\Delta q_c}{Q_R} = \frac{2\Delta q_{c\frac{1}{2}}}{Q_R}\left[\frac{\cos^{-1}\left(2\ \frac{\Delta T}{\Delta T_p} - 1\right)}{90}\right] \tag{12}$$

in terms of q_c, or

$$2\,\Delta z\,\cos\alpha = W\,\frac{2\Delta q_c}{Q_R}\,\frac{\bar{q}}{q_{zp}} \tag{13}$$

in dimensions of length, where q_{zp} = discharge per unit width in portion of channel occupied by plume.

It is implicity assumed in Eqs. 9 - 13 that there is no vertical temperature stratification. Except in the immediate vicinity of the outfall this assumption is judged to be reasonable under most conditions for the Missouri River because of the relatively high velocity, high level of turbulence, and shallow depths in that river.

C. Diffusion Model for Right-Angle Discharge. The transverse temperature distribution function

$$\frac{\Delta T}{\Delta T_p} = \frac{1}{2}\{1 + \cos \pi \zeta\} \tag{14}$$

in Eq. 9, where

$$\zeta = \frac{\Delta q_c}{Q_o\,(\frac{\xi}{\xi_o})^{\frac{1}{2}}},$$

is compared with the Gaussian distribution function

$$\frac{\Delta T}{\Delta T_p} = \exp\,[-\pi\,\zeta^2] \tag{15}$$

in Fig. 5, which shows them to be nearly identical. This property together with the property that $\Delta T_p \propto \xi^{-1/2}$ in Eq. 10 suggests that a diffusion model could be used as an alternative to the modified Carter relationships, exclusive of the trajectory equations. Further investigation showed this to be feasible.

The distribution of temperature rise in the plume, according to the diffusion model, is given by

$$\frac{\Delta T}{\Delta T_o} = \frac{Q_o}{Q_R}\,\frac{1}{2\sqrt{\pi D \xi}}\exp\,[-\frac{p^2}{4D\xi}] \tag{16}$$

where $p = \Delta q_c/Q_R$ and the particular value of the diffusion factor D for which Eq. 16 is essentially equivalent to Eq. 9 is given by

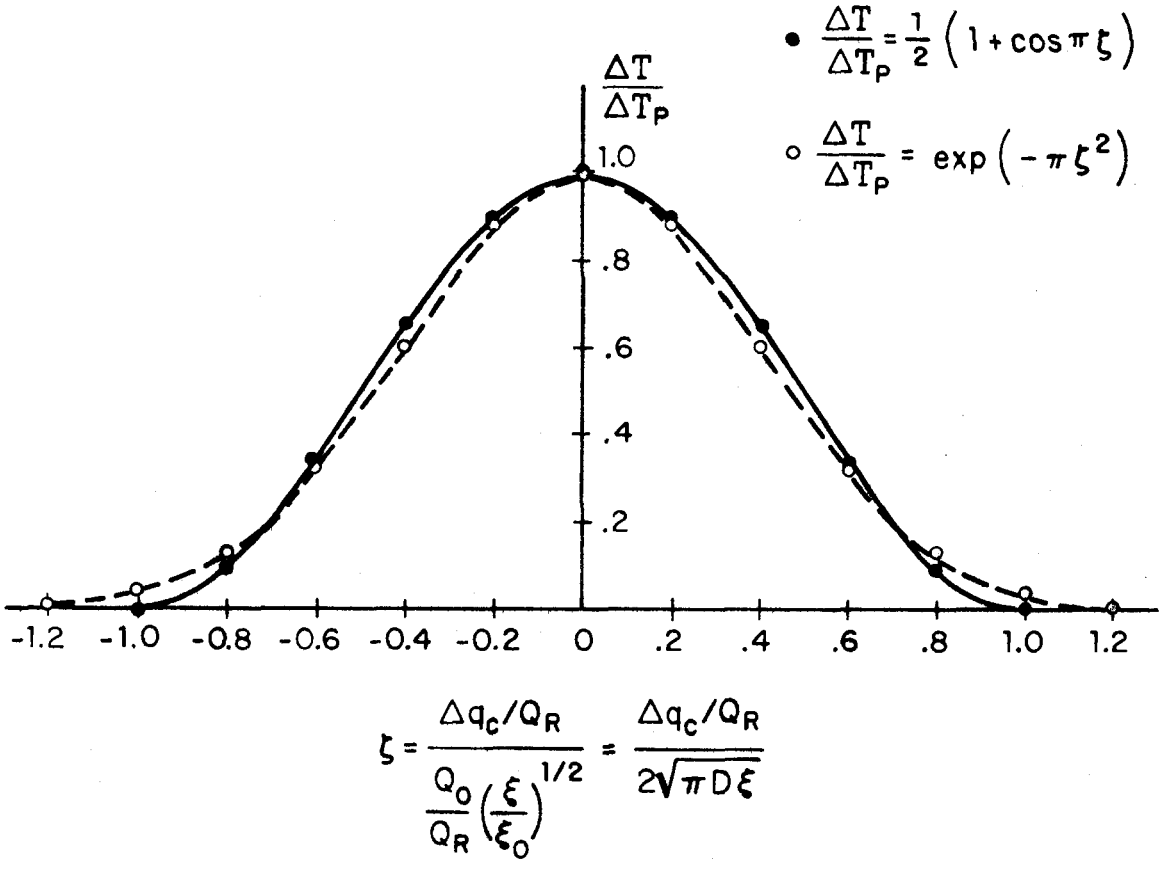

Figure 5. Comparison between transverse distribution of temperature rise given by modified Carter and diffusion models.

$$D_J = \left(\frac{Q_o}{Q_R}\right)^2 / 4\pi\xi_o . \tag{17}$$

The decay of temperature rise along the plume centerline according to the diffusion model is given by

$$\frac{\Delta T_p}{\Delta T_o} = \frac{Q_o}{Q_R} \frac{1}{2\sqrt{\pi D\xi}} . \tag{18}$$

The width of plume within which the temperature rise $\geq \Delta T$ according to the diffusion model is given by

$$2p = 2\{(4D\xi)\ [-\ln\ (\frac{\Delta T}{\Delta T_o} \frac{Q_R}{Q_o} 2\sqrt{\pi D\xi})]\}^{1/2} \tag{19}$$

in terms of p. For the plume width in terms of length dimensions, Eq. 13 with $\Delta q_c/Q_R = p$ applies to the diffusion model also.

Eq. 16 can also be obtained as the solution of the one-dimensional Fickian diffusion equation

$$\frac{\partial\theta}{\partial\xi} = D \frac{\partial^2\theta}{\partial p^2} \tag{20}$$

where $\theta = \Delta T/\Delta T_o$, the dimensionless temperature rise, for the case of a continuous point source of initial temperature rise ΔT_o, discharging at the constant volumetric rate Q_o, and located at $\xi = 0$, $p = 0$.

A particularly attractive feature of the diffusion model is that it facilitates incorporation of the transverse mixing mechanisms associated with the ambient flow into the overall analysis. Sayre and Yeh (7) have demonstrated that the transverse mixing rate of the ambient flow can be quite high in the Missouri River, particularly in bends. Yotsukura and Cobb (12) have shown that a diffusion factor of the type required in Eqs. 16 and 20 can be related to the conventional transverse diffusion coefficient, E_{ZA}, in the diffusion equation for transverse mixing in the ambient flow

$$\bar{U}_A \frac{\partial\theta}{\partial X} = E_{ZA} \frac{\partial^2\theta}{\partial z^2} \tag{21}$$

by the relationship

$$D_A = \frac{\bar{d}\ \bar{q}\ E_{ZA}}{Q_R^2} . \tag{22}$$

As a first approximation it is reasonable to assume that the diffusion factors D_J for the jet-induced mixing and D_A for the ambient flow are independent and therefore additive so that

$$D = D_J + D_A = \frac{\bar{d}\,\bar{q}}{Q_R^2}\,(E_{ZJ} + E_{ZA}). \tag{23}$$

In the present study values of the ambient transverse diffusion coefficient, averaged over the length of a bend, were estimated using the semi-empirical equation

$$\frac{E_{ZA}}{\bar{d}\,U_*} = 1750\,\left(\frac{\bar{U}_A}{U_*}\right)^2\left(\frac{\bar{d}}{r_c}\right)^2 \tag{24}$$

wherein $U_* = \sqrt{g\bar{d}S}$ = shear velocity based on average channel depth, and r_c = radius of curvature of bend. The functional form of Eq. 24 was derived by Fischer (2) in a transverse convective dispersion analysis which utilized Rozovskii's (5) radial velocity distribution function for an idealized curved channel. The numerical coefficient is based on transverse mixing data obtained along the Langdon and Aspinwall bends downstream from the Cooper Nuclear Station (7) at about Mile 530, and along a bend downstream from Blair, Nebraska (13) at about Mile 640 on the Missouri River.

One would expect the jet diffusion factor to decrease due to bottom drag,and the relative importance of the ambient flow diffusion factor to increase going in the downstream direction. However, the Carter et al (1) relationships indicated no such decay, and none was incorporated into the present study.

For the case of a thermal outfall discharging at right angles to the ambient flow it is anticipated that mixing will be quite rapid so that variation of the cross-sectional and ambient flow properties in the longitudinal direction need not be considered. It is considered sufficient to average these properties over the length of the reach in question, and so obtain a composite cross section and corresponding ambient flow properties.

D. Diffusion Model for Parallel Discharge. Due to behavioral differences between plumes resulting from jets that are discharged parallel to and at right angles to the bank, appropriate computational procedures for analyzing these two cases differ in several important respects. First, it is judged that mixing will be much slower, both because the plume will hug the Missouri shore so that entrainment and mixing can occur only along one side of the plume, and also because the entrainment and mixing capacity

of the jet will be reduced still further by boundary drag, not only along the bottom, but also along the shoreward side. Because of the slow mixing rate, longitudinal variations in the properties of the cross-section and the ambient flow can strongly affect the plume pattern. It is therefore necessary to take these longitudinal variations into account. Also, because of the reduced rate of jet mixing, the mixing mechanisms of the ambient flow become relatively more important. Finally, the plume is assumed to be one-sided so that the Missouri shore corresponds to the centerline trajectory for the case of the right angle discharge, whence $\xi = x$ if the Missouri shore is taken as the x axis.

All things considered, the diffusion model, modified so as to permit longitudinal variations in cross-sectional and ambient flow properties was judged to be the most appropriate approach. The modifications are accomplished by dividing the reach of interest into a number of sub-reaches, and the introduction of virtual sources.

Several typical cross sections, numbered 0, 1, 2, ..., i, ..., beginning with section 0 located at the outfall and going in the downstream direction, are selected as control sections. The reaches between successive control sections are designated as subreaches with the i'th subreach extending from the i-1st to the i'th control section. The value of the overall diffusion factor for the i'th reach is taken to be

$$D_i = \frac{\bar{d}_i \, \bar{q}_i \, E_{Z_i}}{Q_R^2} \tag{25}$$

where $\bar{d}_i$, $\bar{q}_i$ and E_{Z_i} are the average values of $\bar{d}$, $\bar{q}$ and $E_Z = E_{ZJ} + E_{ZA}$ for the i-1'st and i'th control sections.

The temperature-rise distribution in the i'th subreach is given by

$$\frac{\Delta T}{\Delta T_o} = \frac{Q_o}{Q_R} \frac{1}{\sqrt{\pi D_i (x - x_{o_i})}} \exp\left[- \frac{p^2}{4 D_i (x - x_{o_i})} \right] \tag{26}$$

where $p = q_c/Q_R$, since $\Delta q_c = q_c$ because $q_{cp} = 0$, and x_{o_i} = longitudinal coordinate of virtual source for i'th subreach. In order to have a continuous function from subreach to subreach the condition

$$D_i \, (x_{i-1} - x_{o_i}) = D_{i-1} \, (x_{i-1} - x_{oi-1}), \tag{27}$$

where x_{i-1} = x at upstream end of i'th subreach = x at downstream end of i-1st subreach, is imposed on the virtual sources. Starting with $x_{o_i} = 0$, Eq. 27 is used recursively to compute the virtual source locations for the successive subreaches.

The decay of the peak temperature rise along the Missouri shore according to Eq. 26 is given by

$$\frac{\Delta T_p}{\Delta T_o} = \frac{Q_o}{Q_R} \frac{1}{\sqrt{\pi D_i (x-x_{o_i})}} \tag{28}$$

The width of plume within which the temperature rise $\geq \Delta T$ is given by

$$p = \{ 4D_i (x-x_{o_i}) [-\ln(\frac{\Delta T}{\Delta T_o} \frac{Q_R}{Q_o} \sqrt{\pi D_i (x-x_{o_i})})] \}^{1/2} \tag{29}$$

in terms of p.

The transverse diffusion coefficient for jet-induced mixing in the parallel discharge case is estimated by the equation

$$E_{ZJ_i} = \frac{Q_R^2 D_J}{\bar{d}_i \bar{q}_i} = \frac{Q_o^2}{4\pi \bar{d}_i \bar{q}_i \xi_o} \tag{30}$$

where

$$\xi_o = 20 b_o . \tag{31}$$

Eq. 31 was obtained by assuming that the rate of dilution induced by the parallel jet is one-half that induced by the two-dimensional right-angle jet in the Carter et al (1) relationships. This corresponds to roughly one-fourth to one-third of the dilution rate for the right-angle jet in this study.

IV. PRESENTATION OF PREDICTED TEMPERATURE DISTRIBUTIONS

A. Supporting Data. The composite cross sections, together with the synthesized transverse distributions of $q/\bar{q}$ and q_c/Q_R, that were used in predicting the temperature rise distributions for the right-angle discharge are shown in Figs. 6a - 6c for Q_R = 35,000, 20,000 and 10,000 cfs, respectively. The properties of the composite section were

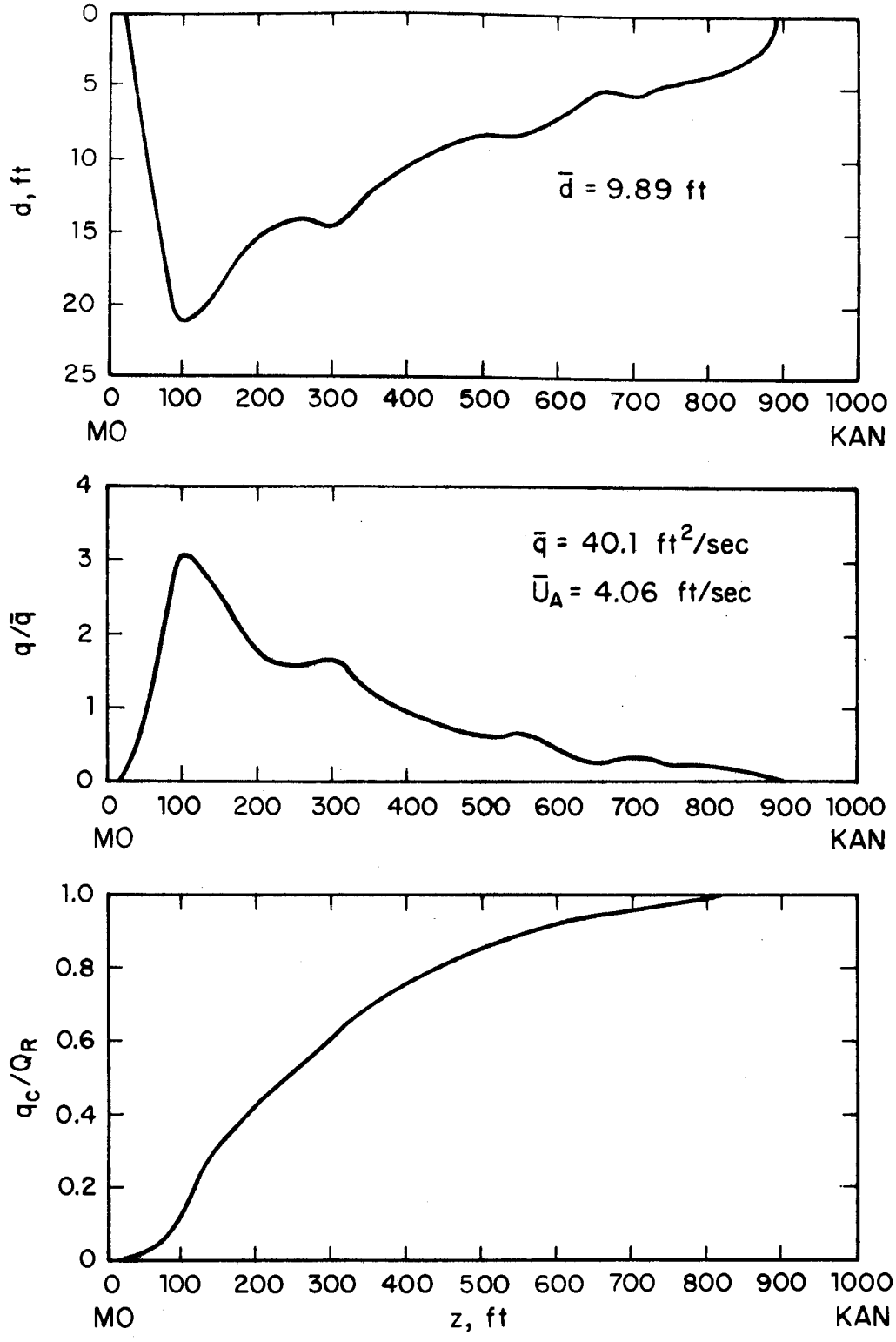

Figure 6a. Synthesized distribution of depth, unit discharge, and cumulative discharge in composite section for Q_R = 35,000 cfs.

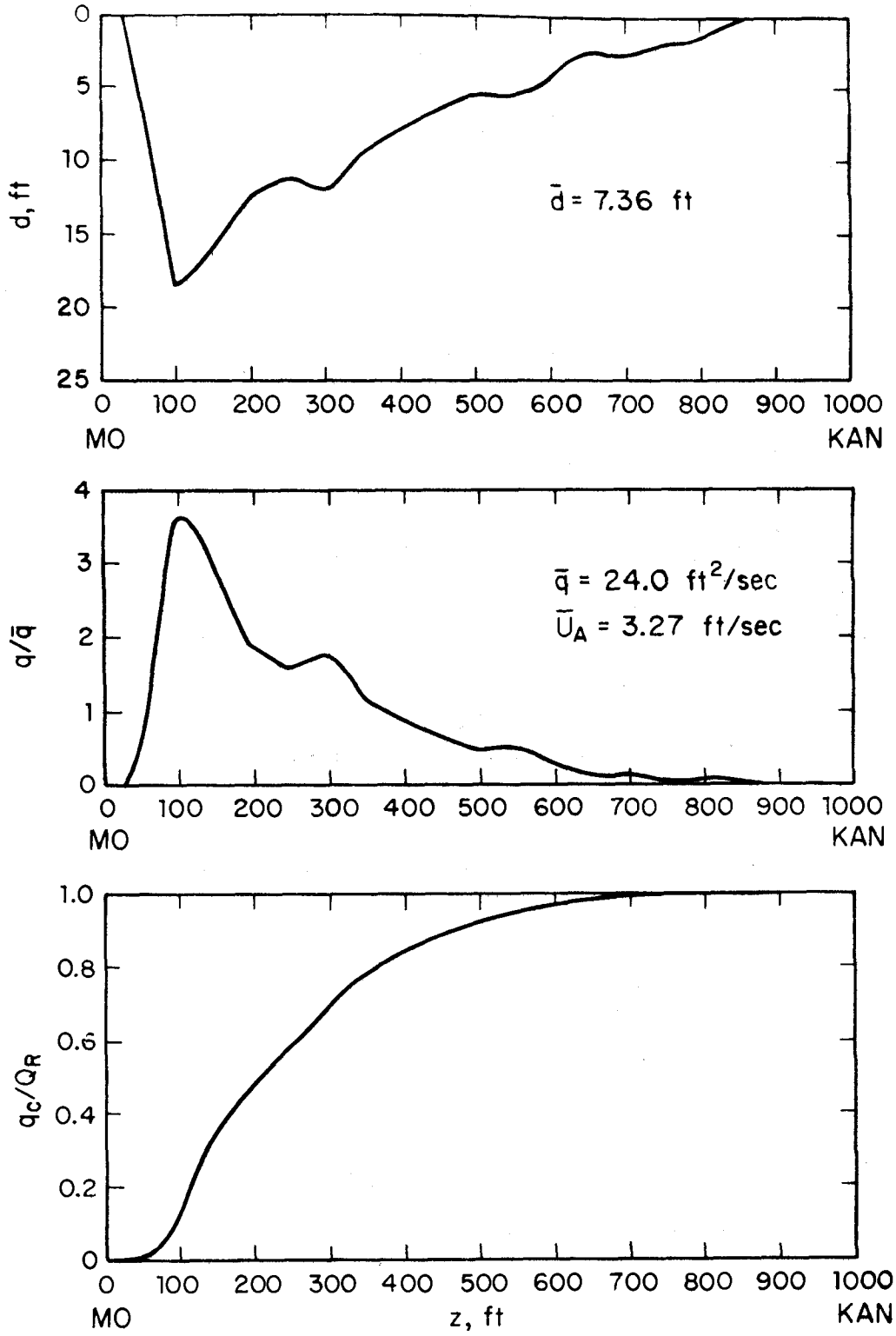

Figure 6b. Sythesized distribution of depth, unit discharge, and cumulative discharge in composite section for Q_R = 20,000 cfs.

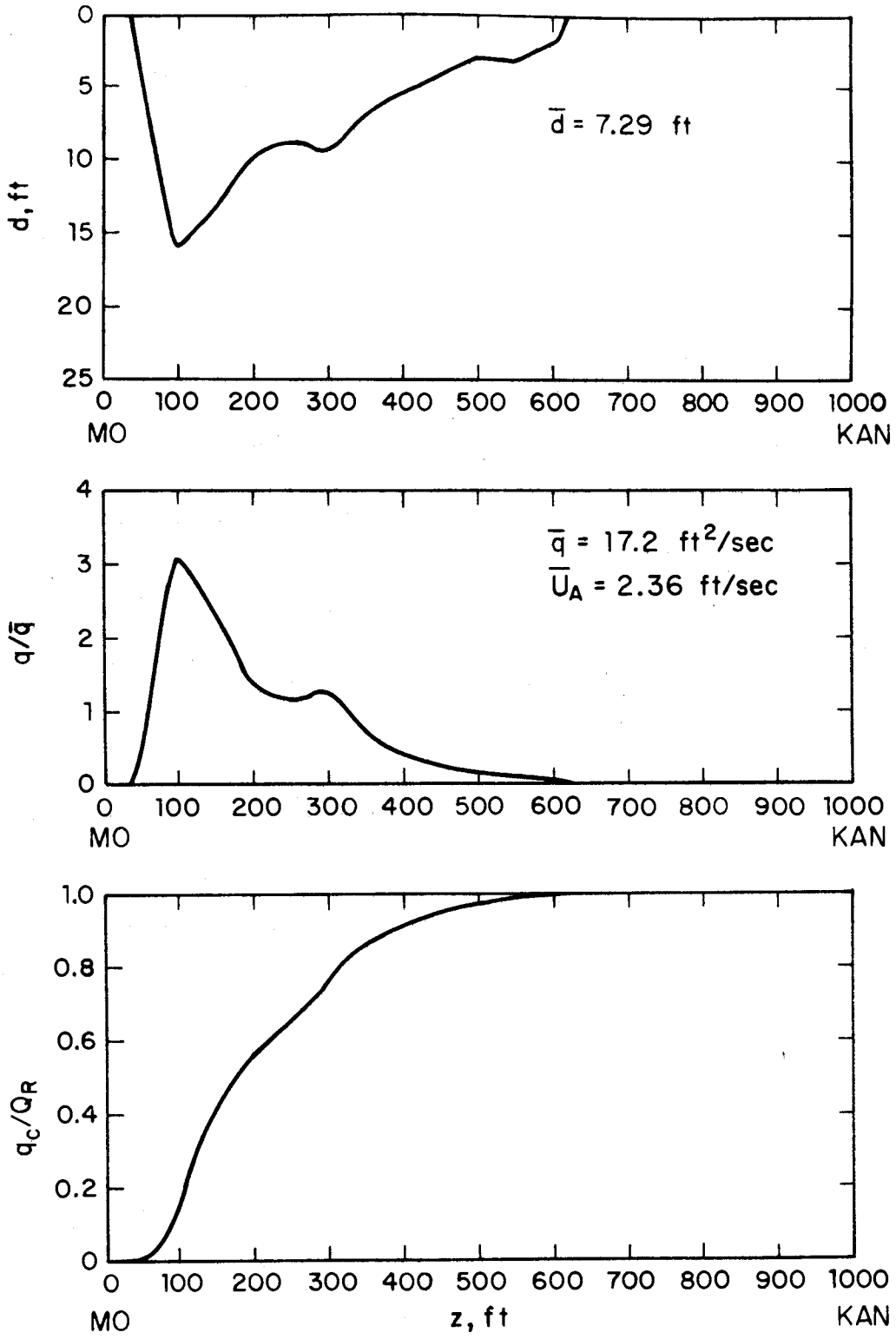

Figure 6c. Synthesized distribution of depth, unit discharge, and cumulative discharge in composite section for Q_R = 10,000 cfs.

obtained by averaging four cross sections located between mile 411.2 and 410.9. The cross sections were determined from depth sounding data reported in the Corps of Engineers November 1972 Hydrographic Survey (9). No dramatic change in the shape or size of the cross section occurs until about Mile 410.

Table 3 lists properties and parameters describing the ambient and initial jet flows that were used in the thermal plume calculations for the right-angle discharge. The opposite trends in the values of the transverse diffusion coefficients E_{ZA} and E_{ZJ} for the ambient flow and the jet in Cols. 11 and 12 with respect to river discharge are particularly significant. The increase in E_{ZJ} as Q_R is reduced is due mainly to the increase in initial jet velocity U_o which accompanies the drop in river stage.

For both the right-angle and parallel jet discharges, the configuration of the outfall structure at the point of discharge is assumed to be an 8-ft wide rectangular slot with a bottom elevation of 748.8 ft above mean sea level.

The nine cross sections used as control sections in the parallel discharge analysis are shown in Figs. 7a - 7c. With the exception of Section 2 for which the USGS data shown in Fig. 2c was used, the data for the control sections was taken from the Corps of Engineers November 1972 Hydrographic Survey (9). A cursory examination of the channel shapes shows that the thalweg shifts from the Missouri side at Mile 411.2, over to the Kansas side at Mile 409.2, back to the Missouri side at Mile 407.6, and over to the Kansas side again at Mile 406.0. This type of pattern, with the thalweg hugging the outside of the bends, is typical for sinuous and meandering alluvial channels.

Synthesized q_c/Q_R versus z/W curves for Q_R = 35,000, 20,000 and 10,000 cfs are shown in Figs. 8a - 8i for the same nine control sections.

Table 4 lists the properties and parameters of the control sections that were used to calculate the properties and parameters of the subreaches listed in Table 5, which in turn were used in the thermal plume calculations. Comparison of Cols. 10 and 11 in Table 4 shows that ambient transverse diffusion tends to be dominant for Q_R = 35,000 and 20,000 cfs, whereas the transverse diffusion attributable to the jet tends to be dominant when Q_R = 10,000 cfs.

Table 3. BACKGROUND DATA DESCRIBING COMPOSITE CROSS SECTION, AND PARAMETERS USED IN PLUME CALCULATIONS FOR RIGHT-ANGLE DISCHARGE

River Discharge	Channel Width	Average Depth	Average Ambient Velocity	Average Discharge per Unit Width	Shear Velocity	Initial Jet Height	Initial Jet Velocity	Velocity Ratio	Flow Establishment Distance	Ambient Transverse Diffusion Coefficient	Jet Transverse Diffusion Coefficient	Overall Diffusion Factor
Q_R	W	$\bar{d}$	$\bar{U}_A$	$\bar{q}$	U_*	h_o	U_o	$R=\frac{U_o}{\bar{U}_A}$	ξ_o	E_{ZA}	E_{ZJ}	$Dx10^6$
cfs	ft	ft	ft/sec	ft^2/sec	ft/sec	ft	ft/sec		ft	ft^2/sec	ft^2/sec	ft^{-1}
(1)	(2)	(3)	(4)	(5)	(6)	(7)	(8)	(9)	(10)	(11)	(12)	(13)
35,000	872	9.9	4.1	40.1	0.247	15.1	6.18	1.51	55.0	1.86	2.03	1.2
20,000	832	7.4	3.3	24.0	0.213	12.2	7.64	2.32	49.4	0.58	5.08	2.51
10,000	582	7.3	2.4	17.2	0.212	9.7	9.61	4.00	44.0	0.29	8.03	10.45

Initial Temperature Rise $\Delta T_o = 18.7°F$

Jet Discharge $Q_o = 746$ cfs

Initial Jet Width $b_o = 8$ ft

Radius of Curvature of Bend $r_c = 7{,}800$ ft

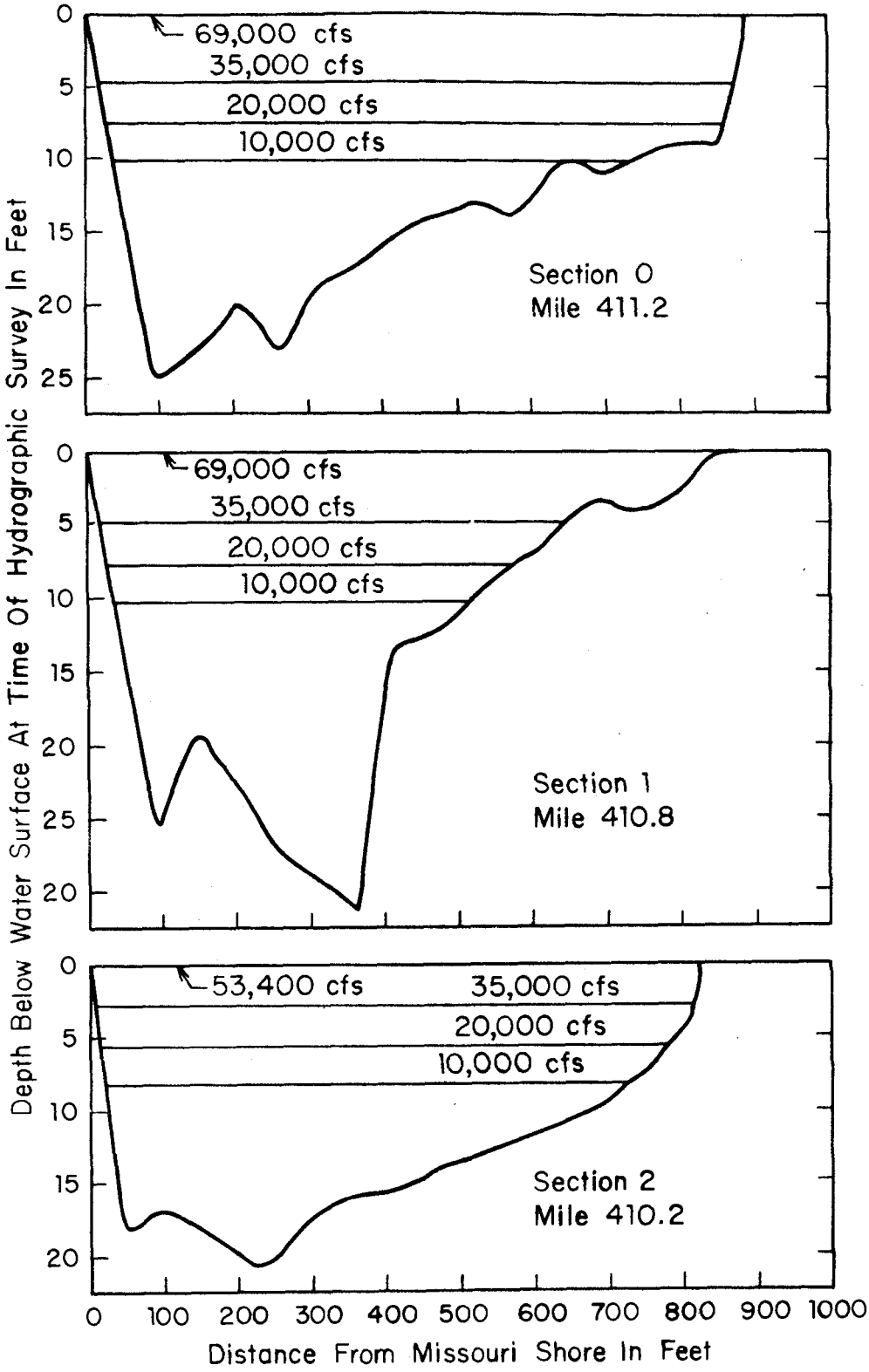

Figure 7a. Transverse bed profiles for control sections 0, 1 and 2.

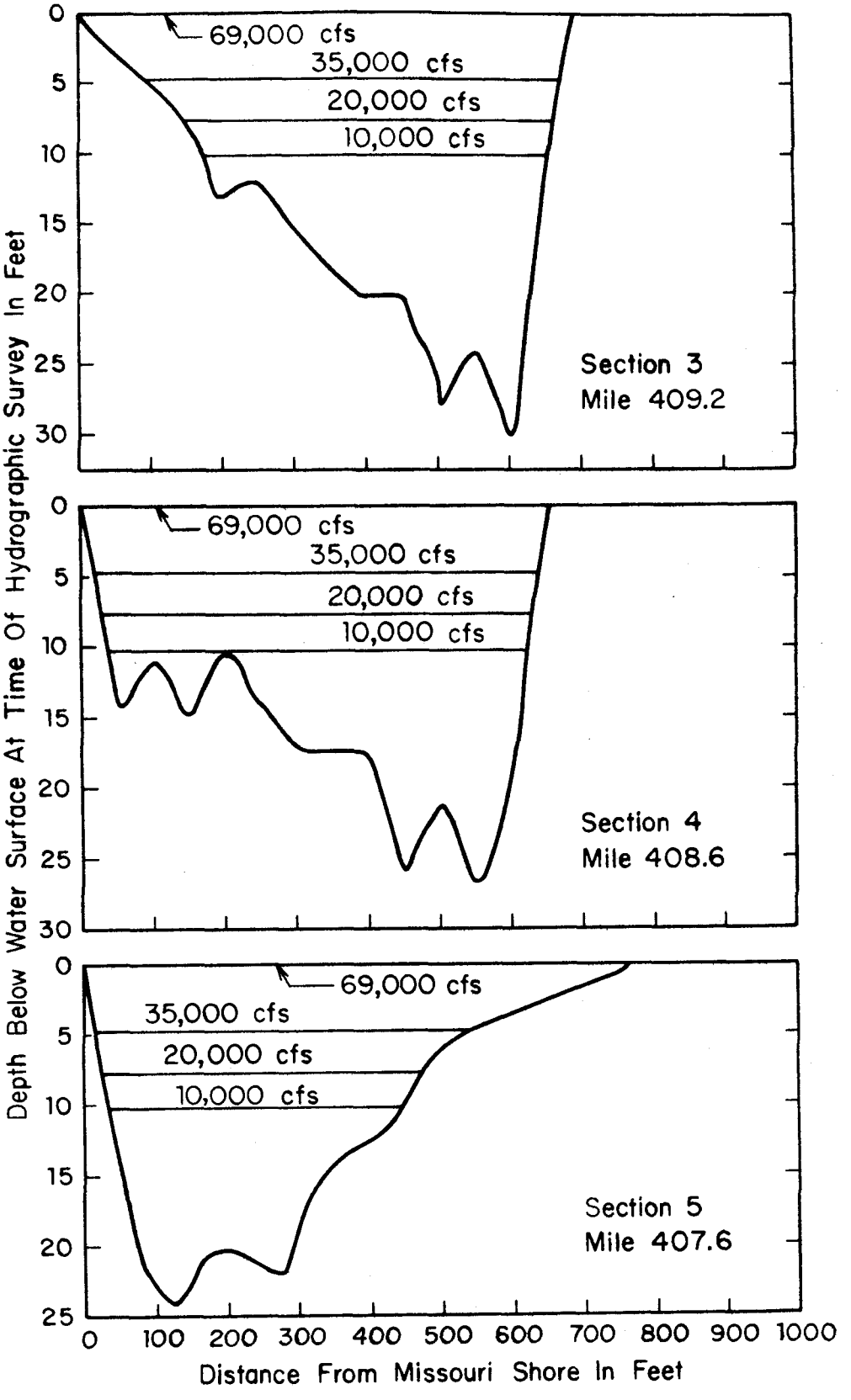

Figure 7b. Transverse bed profiles for control sections 3,4 and 5.

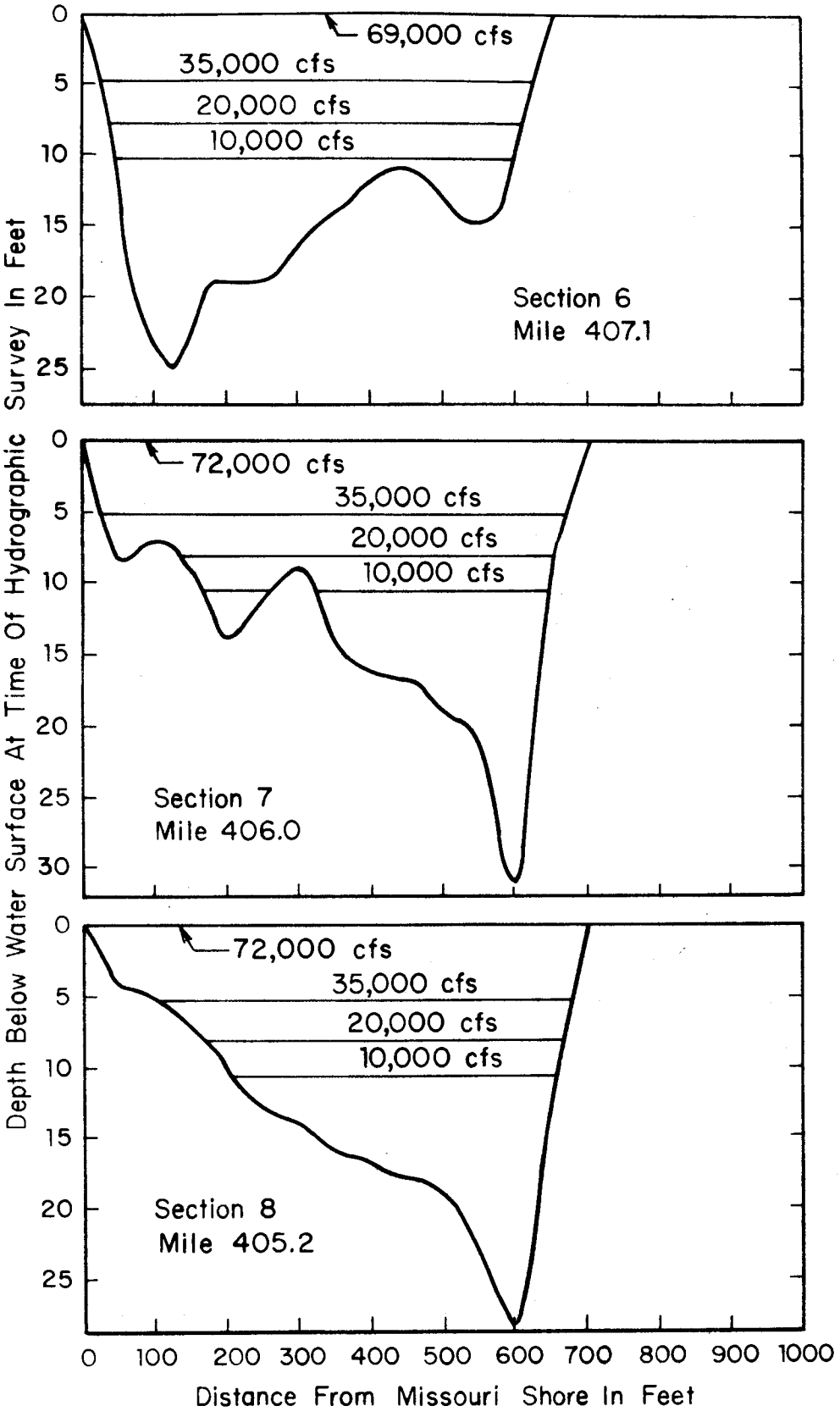

Figure 7c. Transverse bed profiles for control sections 6,7 and 8.

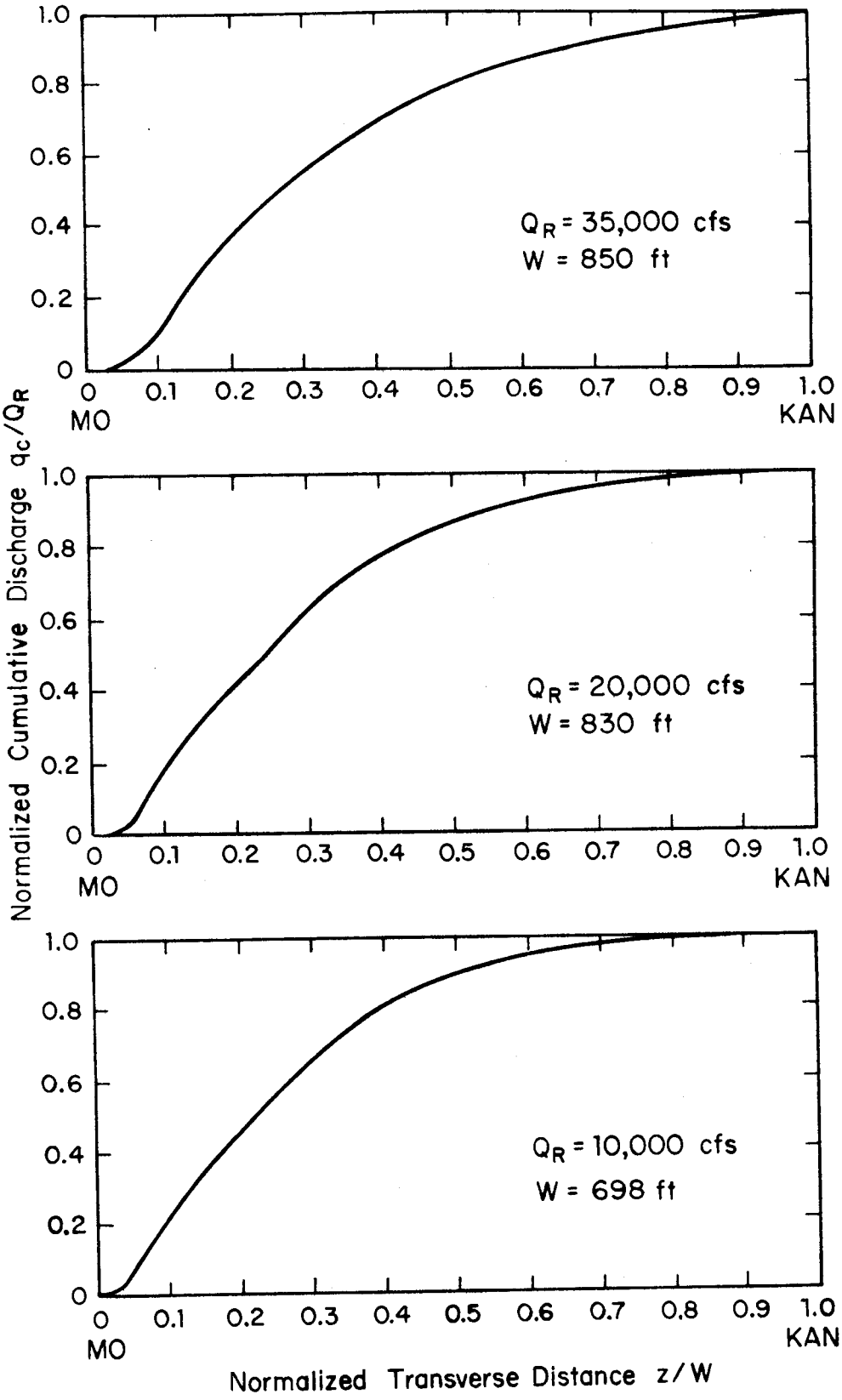

Figure 8a. Normalized cumulative discharge curves for section O at Mile 411.2.

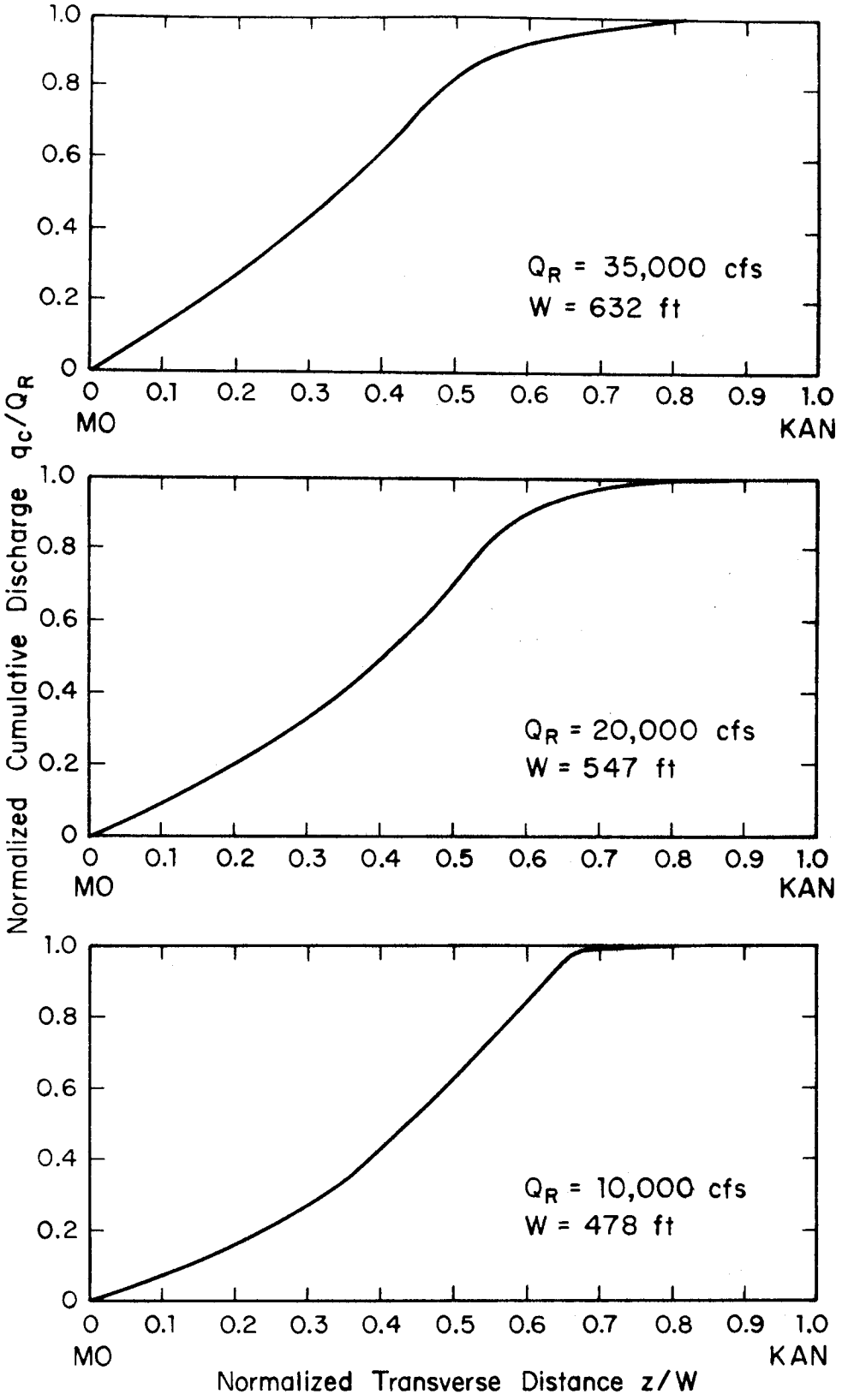

Figure 8b. Normalized cumulative discharge curves for Section 1 at Mile 410.8.

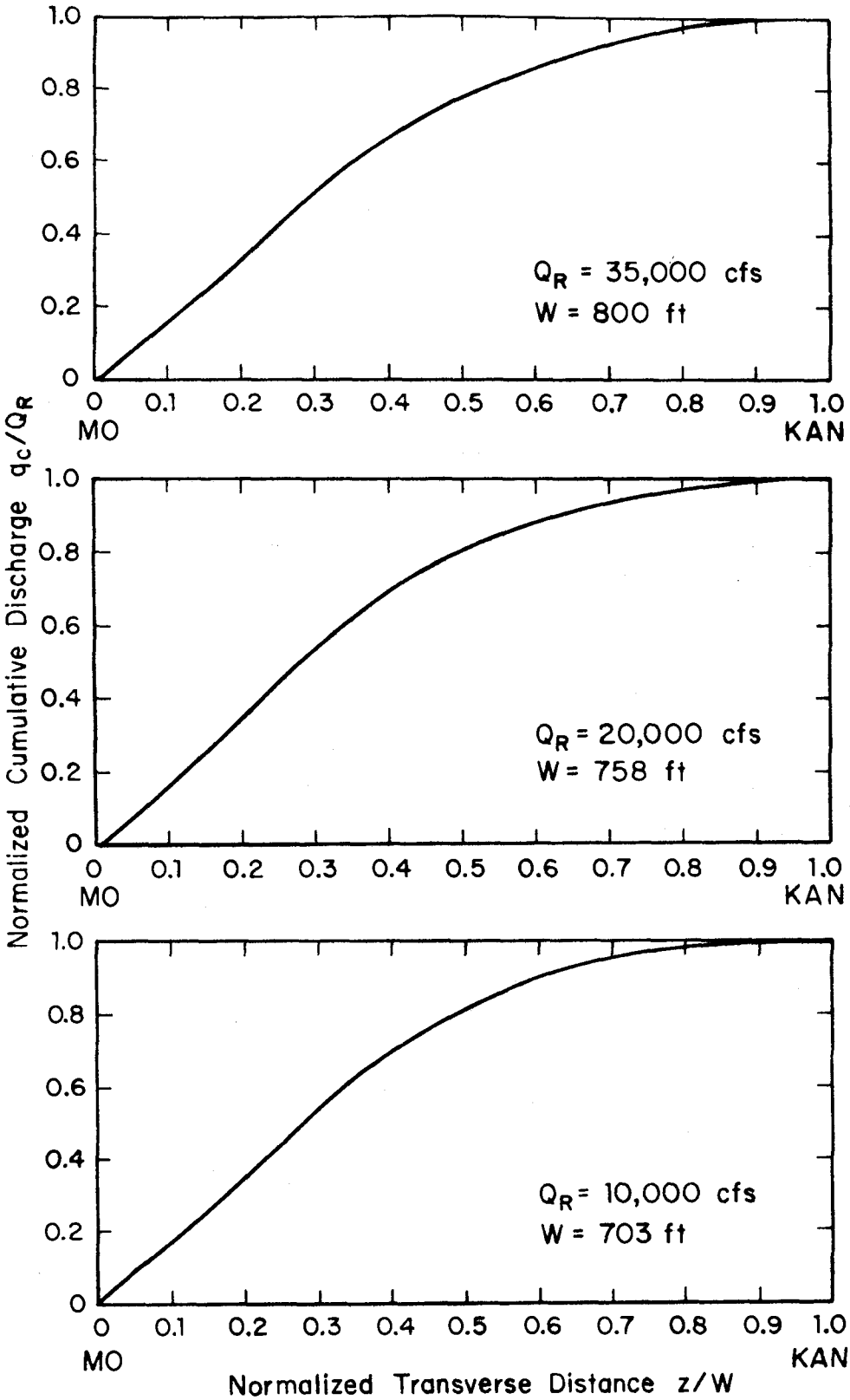

Figure 8c. Normalized cumulative discharge curves for Section 2 at Mile 410.2.

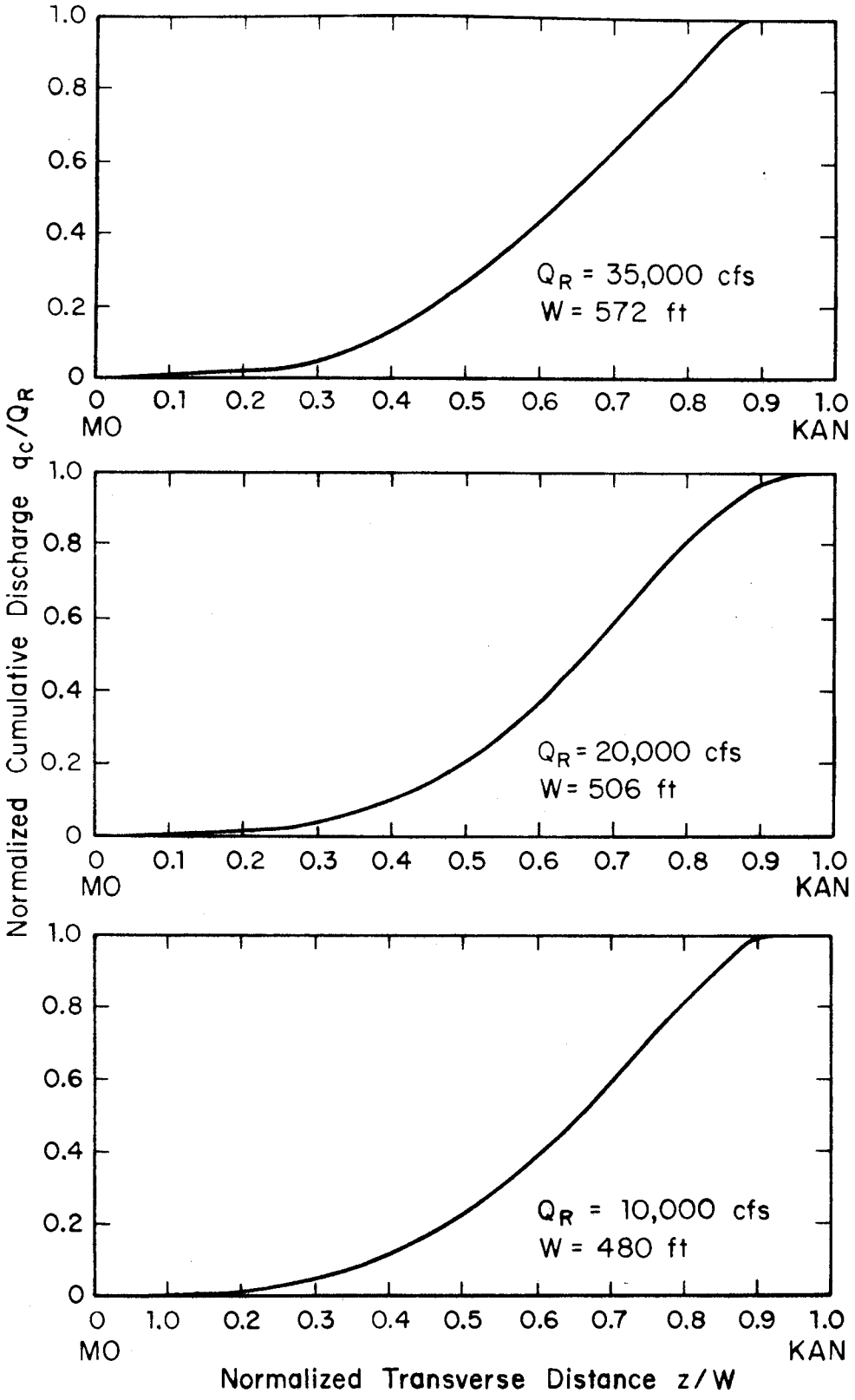

Figure 8d. Normalized cumulative discharge curves for Section 3 at Mile 409.2.

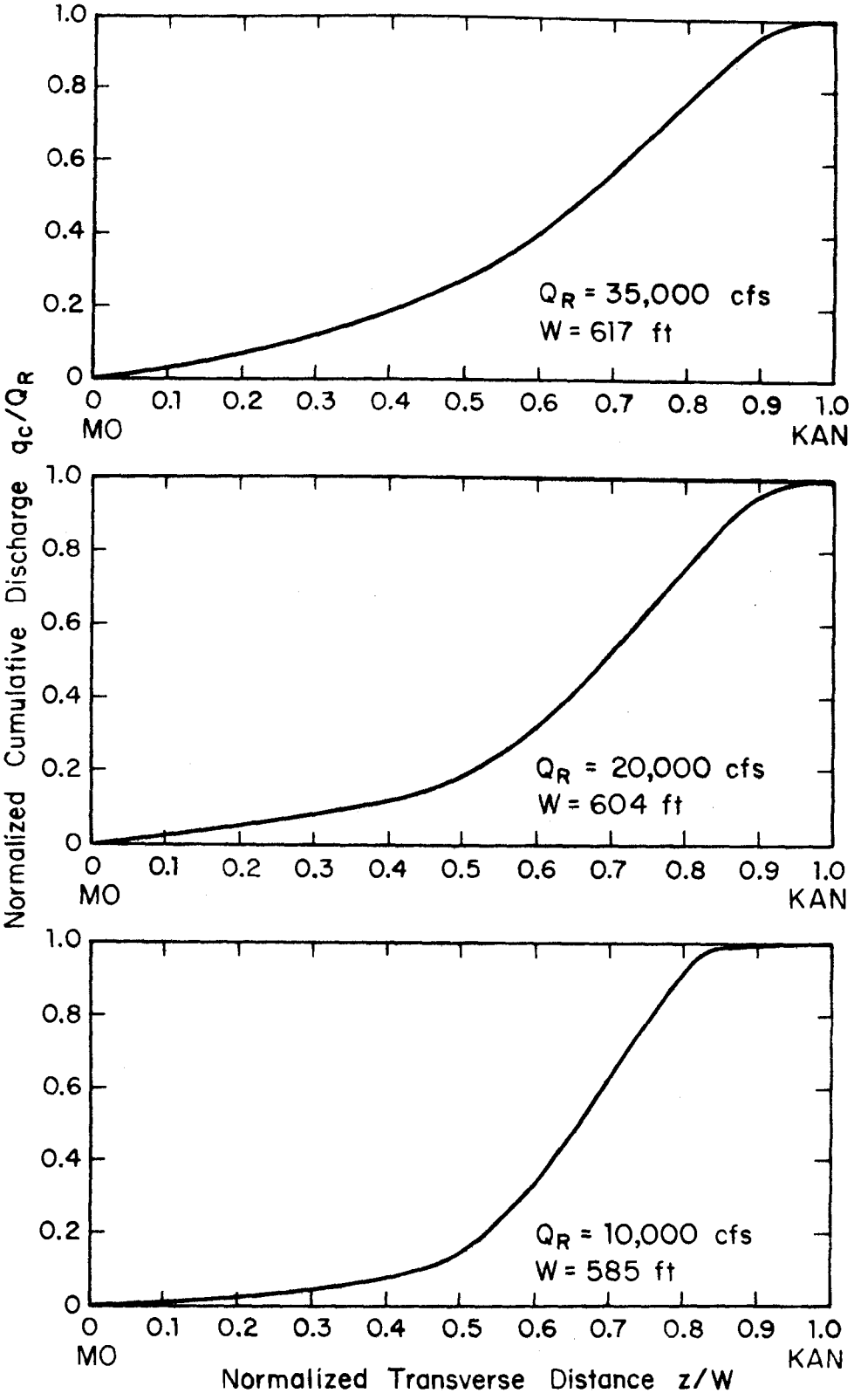

Figure 8e. Normalized cumulative discharge curves for Section 4 at Mile 408.6.

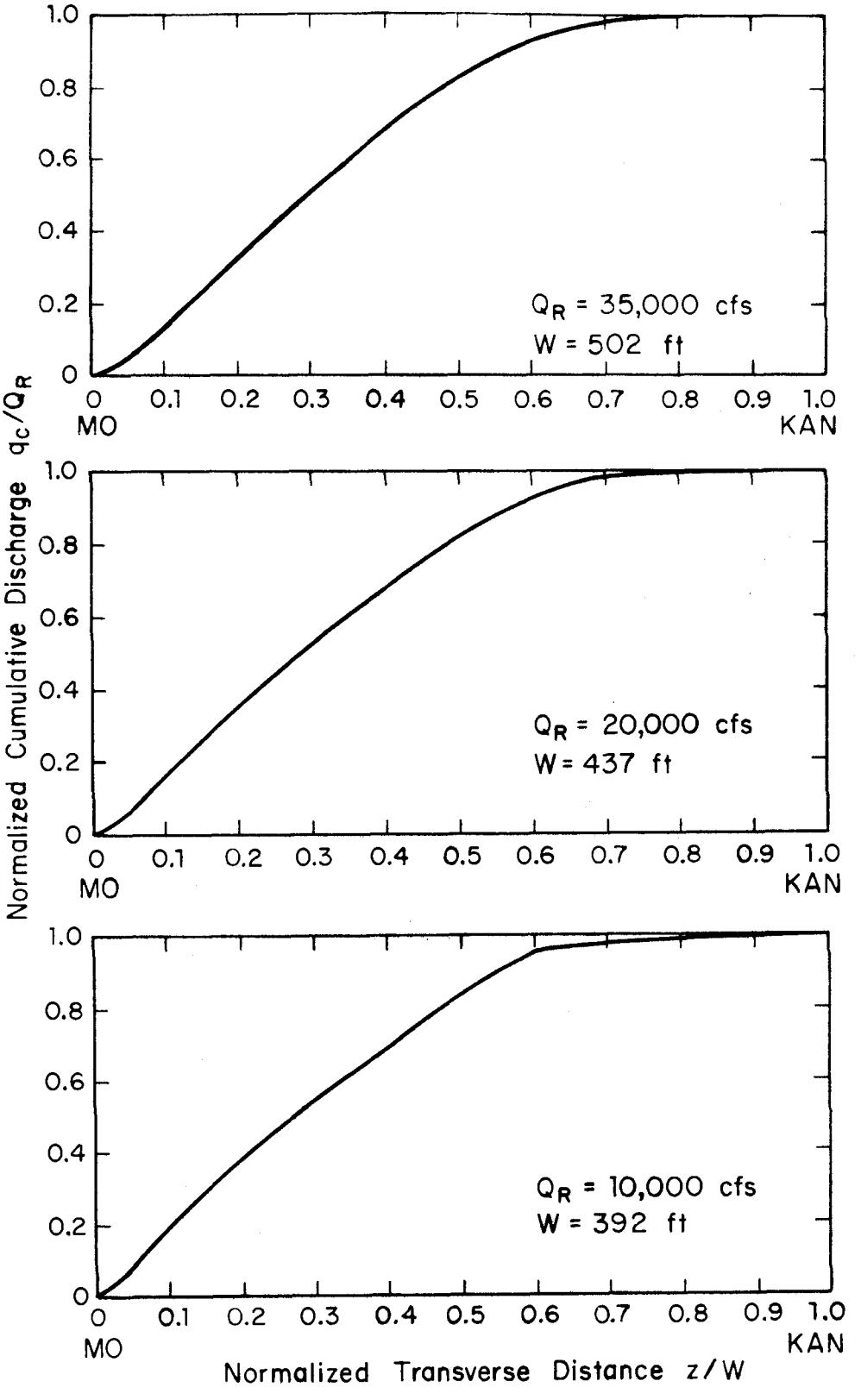

Figure 8f. Normalized cumulative discharge curves for Section 5 at Mile 407.6.

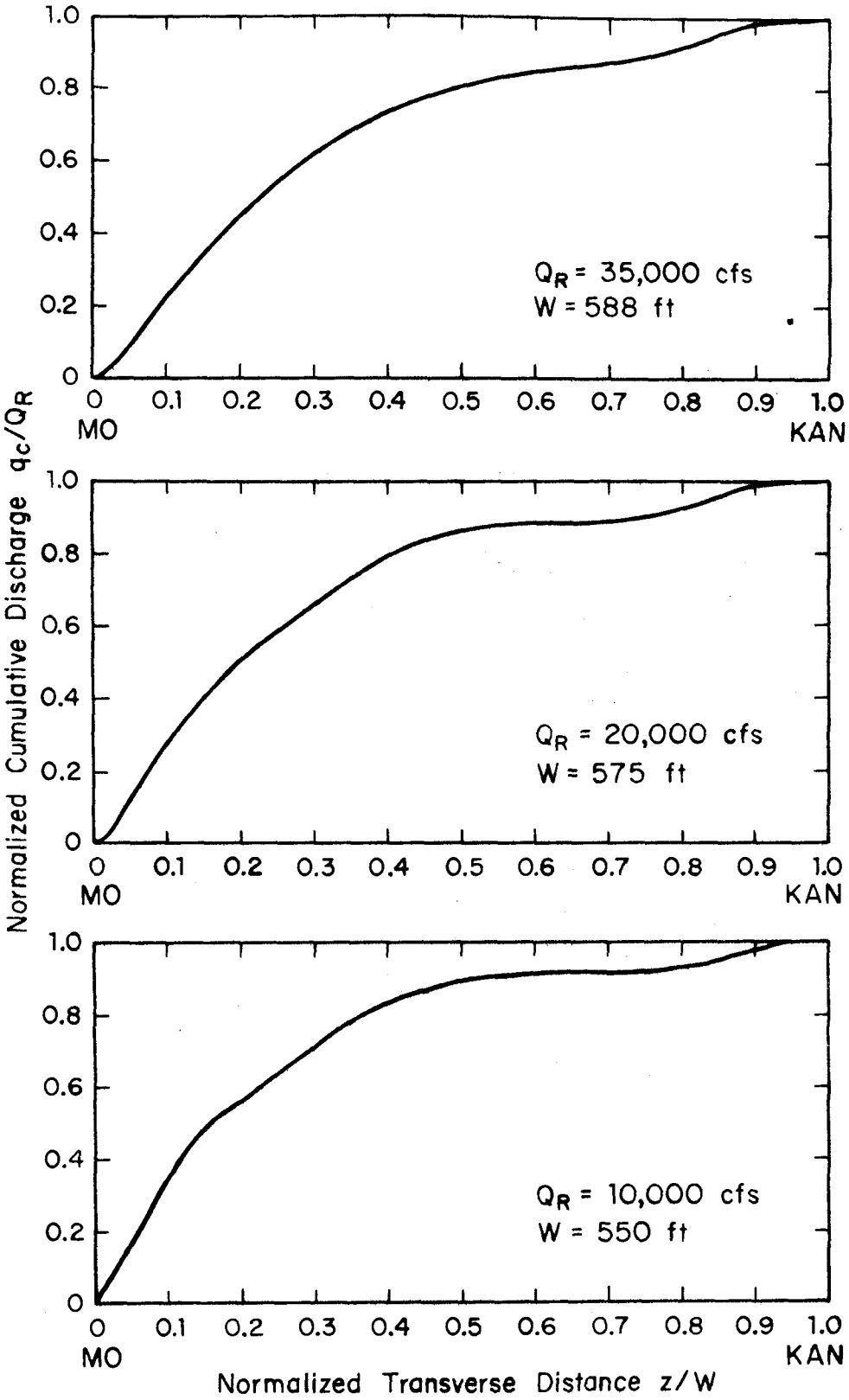

Figure 8g. Normalized cumulative discharge curves for Section 6 at Mile 407.1.

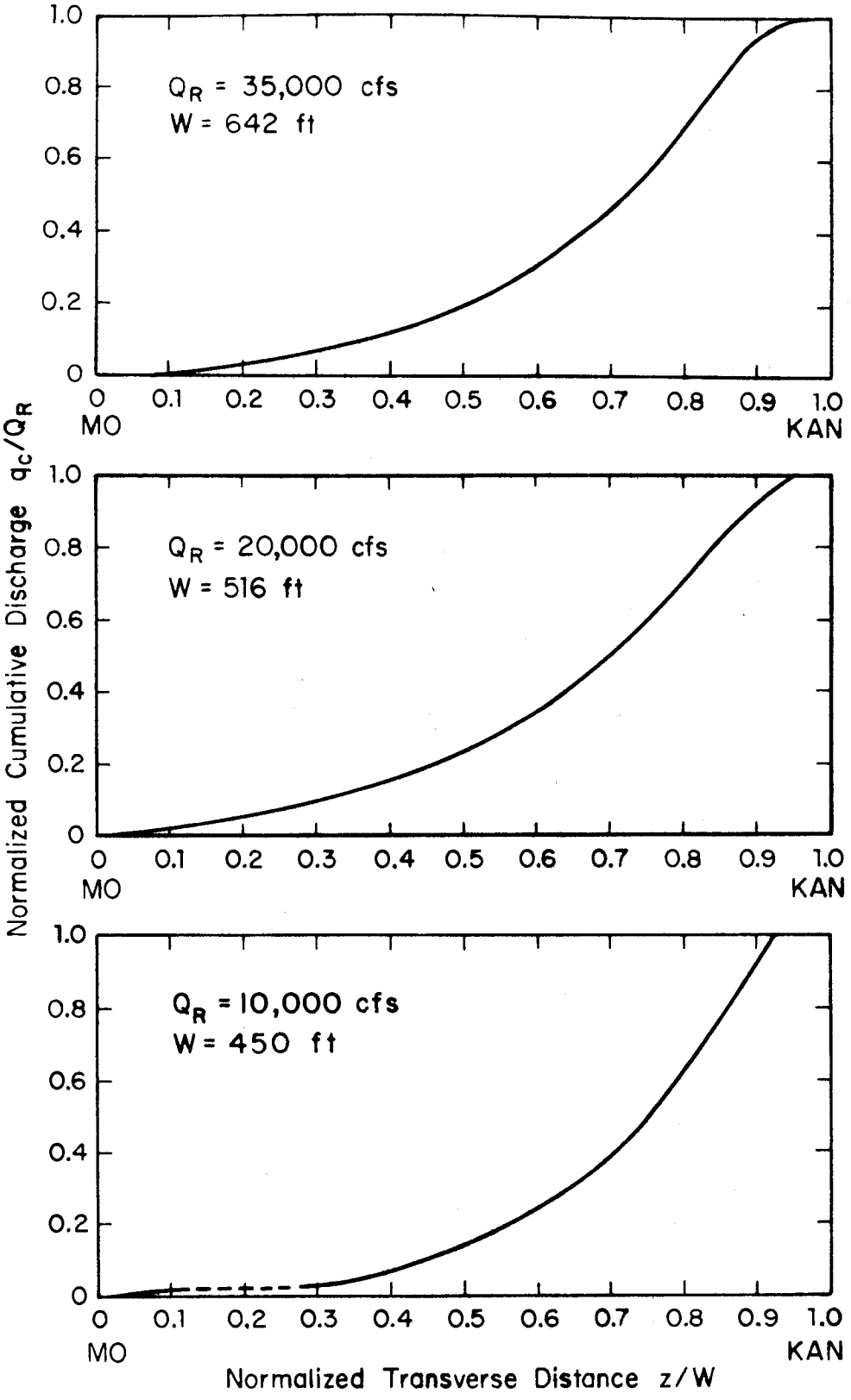

Figure 8h. Normalized cumulative discharge curves for Section 7 at Mile 406.0.

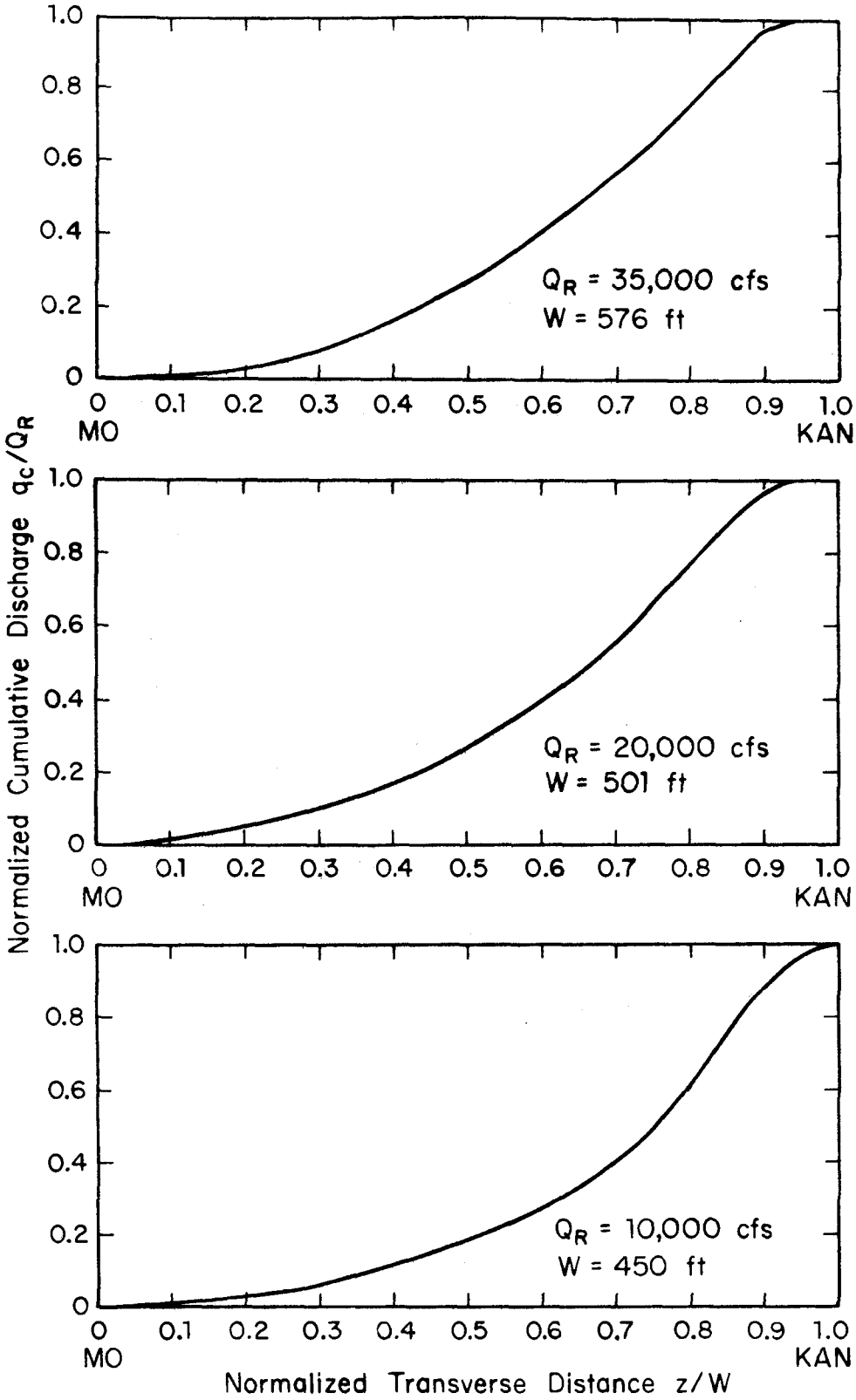

Figure 8i. Normalized cumulative discharge curves for Section 8 at Mile 405.2.

Table 4. BACKGROUND DATA DESCRIBING CONTROL SECTIONS AND PARAMETERS USED IN PLUME CALCULATIONS FOR PARALLEL DISCHARGE

River Discharge	Section	Downstream Distance	Channel Width	Average Depth	Average Ambient Velocity	Average Discharge per Unit Width	Shear Velocity	Radius of Bend	Ambient Transverse Diffusion Coeffic-ent	Jet Transverse Diffusion Coeffic-ent	Overall Transverse Diffusion Coeffic-ent
Q_R		x	W	$\bar{d}$	$\bar{U}_A$	$\bar{q}$	U_*	r_c	E_{ZA}	E_{ZJ}	E_Z
cfs		ft	ft	ft	ft/sec	ft^2/sec	ft/sec	ft	ft^2/sec	ft^2/sec	ft^2/sec
(1)	(2)	(3)	(4)	(5)	(6)	(7)	(8)	(9)	(10)	(11)	(12)
35,000	0	0	850	10.5	3.9	41.2	0.254	7800	2.00	0.64	2.64
	1	2100	632	13.1	4.2	55.4	0.284	7800	4.05	0.38	4.43
	2	5300	800	11.2	3.9	43.8	0.262	7800	2.38	0.56	2.94
	3	10600	572	12.5	4.9	61.2	0.277	6500	6.99	0.36	7.35
	4	13700	617	11.5	5.0	56.7	0.266	6500	5.78	0.42	6.20
	5	19000	502	11.4	6.1	69.7	0.265	4900	15.3	0.35	15.6
	6	21600	588	11.1	5.4	59.5	0.261	4900	11.1	0.42	11.5
	7	27500	642	9.2	5.9	54.5	0.238	6000	5.54	0.55	6.09
	8	31700	576	10.2	6.0	60.8	0.250	6000	7.34	0.45	7.79
20,000	0	0	830	7.8	3.1	24.1	0.219	7800	0.60	1.47	2.07
	1	2100	547	12.0	3.0	36.6	0.272	7800	1.70	0.63	2.33
	2	5300	758	8.9	3.0	26.4	0.234	7800	0.77	1.18	1.95
	3	10600	506	11.2	3.5	39.5	0.262	6500	2.79	0.63	3.42
	4	13700	604	8.9	3.7	33.1	0.234	6500	1.73	0.94	2.67
	5	19000	437	10.0	4.6	45.8	0.248	4900	6.20	0.60	6.80
	6	21600	575	8.4	4.1	34.8	0.227	4900	3.24	0.95	4.19
	7	27500	516	8.1	4.8	38.8	0.223	6000	2.69	0.88	3.57
	8	31700	501	8.6	4.6	39.9	0.230	6000	2.87	0.81	3.68

Table 4. Continued-

(1)	(2)	(3)	(4)	(5)	(6)	(7)	(8)	(9)	(10)	(11)	(12)
10,000	0	0	698	6.7	2.2	14.3	0.203	7800	0.20	2.88	3.08
↓	1	2100	478	11.1	1.9	20.9	0.261	7800	0.55	1.19	1.74
	2	5300	703	7.0	2.0	14.2	0.207	7800	0.20	2.78	2.98
	3	10600	480	9.4	2.2	20.8	0.240	6500	0.70	1.42	2.12
	4	13700	585	6.9	2.5	17.1	0.206	6500	0.41	2.35	2.76
	5	19000	392	8.3	3.1	25.5	0.226	4900	1.73	1.31	3.04
	6	21600	550	6.2	2.9	18.2	0.195	4900	0.77	2.45	3.22
	7	27500	450	7.0	3.2	22.2	0.207	6000	0.80	1.78	2.58
	8	31700	450	7.0	3.2	22.2	0.207	6000	0.81	1.78	2.59

Initial Temperature Rise $\Delta T_o = 18.7°F$

Jet Discharge $Q_o = 746$ cfs

Initial Jet Width $b_o = 8$ ft

Table 5. BACKGROUND DATA AND PARAMETERS FOR SUBREACHES USED IN PLUME CALCULATIONS FOR PARALLEL DISCHARGES

River Discharge	Sub-reach	Sub-reach Number	Overall Transverse Diffusion Coefficient	Average Depth	Average Discharge per Unit Width	Overall Diffusion Factor	Downstream Distance to End of Reach	Virtual Source
Q_R		i	E_{Z_i}	$\bar{d}_i$	$\bar{q}_i$	$D_i X 10^6$	x_i	x_{oi}
cfs			ft^2/sec	ft	ft^2/sec	ft^{-1}	ft	ft
(1)	(2)	(3)	(4)	(5)	(6)	(7)	(8)	(9)
35,000	0-1	1	3.54	11.8	48.3	1.65	2,100	0
	1-2	2	3.69	12.1	49.6	1.81	5,300	186
	2-3	3	5.14	11.8	52.5	2.60	10,600	1,740
	3-4	4	6.77	12.0	59.0	3.91	13,700	4,708
	4-5	5	10.9	11.4	63.2	6.41	19,000	8,215
	5-6	6	13.6	11.2	64.6	8.03	21,600	10,391
	6-7	7	8.80	10.2	57.0	4.18	27,500	67
↓	7-8	8	6.94	9.7	57.7	3.17	31,700	-8,673
20,000	0-1	1	2.20	9.9	30.4	1.66	2,100	0
	1-2	2	2.14	10.4	31.5	1.75	5,300	108
	2-3	3	2.69	10.0	33.0	2.22	10,600	1,207
	3-4	4	3.05	10.0	36.3	2.77	13,700	3,072
	4-5	5	4.74	9.4	39.5	4.40	19,000	7,009
	5-6	6	5.50	9.2	40.3	5.10	21,600	8,655
	6-7	7	3.88	8.2	36.8	2.93	27,500	-932
↓	7-8	8	3.63	8.3	39.4	2.97	31,700	-549

Table 5. Continued-

(1)	(2)	(3)	(4)	(5)	(6)	(7)	(8)	(9)
10,000	0-1	1	2.41	8.9	17.6	3.78	2,100	0
↓	1-2	2	2.36	9.0	17.6	3.74	5,300	-22
	2-3	3	2.55	8.2	17.5	3.66	10,600	-138
	3-4	4	2.44	8.2	19.0	3.80	13,700	258
	4-5	5	2.90	7.6	21.3	4.69	19,000	2,809
	5-6	6	3.13	7.3	21.9	5.00	21,600	3,813
	6-7	7	2.90	6.6	20.2	3.87	27,500	-1,381
	7-8	8	2.59	7.0	22.2	4.02	31,700	-303

Initial Temperature Rise $\Delta T_o = 18.7°F$

Jet Discharge $Q_o = 746$ cfs

Initial Jet Width $b_o = 8$ ft

B. Results for Right-Angle Discharge. Fig. 9 shows sets of 5°F (2.8°C) and 1.8°F (1°C) temperature-rise isotherms for the three river discharges. The locations of the 10°F isotherms were also calculated, but the 10°F isotherms enclosed too small a region to plot. Corresponding transverse temperature-rise distributions are shown for distances 500, 1,000, 2,000 and 5,000 downstream from the outfall in Figs. 10a - 10c. The river cross section is shown underneath so that the association between temperature rise and the portions of the channel that are affected can be seen. The Missouri shore was treated as a reflecting boundary.

The temperature-rise isotherms in Fig. 9 and transverse distribution profiles in Figs. 10a - 10c were predicted using the diffusion model, Eqs. 16 - 19, in conjunction with the modified Carter centerline trajectory for a three-dimensional jet given in Eqs.7 and 8. The decision to use the three-dimensional rather than the two-dimensional trajectory, which carries significantly further out into the river, was influenced by results being obtained in a current model investigation at the Iowa Institute of Hydraulic Research, in which the performance of a right-angle rectangular slot-jet structure for Unit 1 of the Dresden Nuclear Station that discharges into the Illinois River is being investigated. Centerline trajectories observed in the model are being found to agree far better with the trajectory equations for the three-dimensional jet.

The set of isotherms in Fig. 11 is shown for comparison. They were predicted using the modified Carter et al relationships, Eqs. 9 - 13, without including ambient transverse diffusion, in conjunction with the centerline trajectory for the two-dimensional jet given in Eqs. 5 and 6. Comparing the isotherms in Figs. 9 and 11, exclusion of ambient transverse diffusion has a major effect on the isotherms for Q_R = 35,000 cfs in Fig. 11, but a small effect on the isotherms for Q_R = 20,000 and 10,000 cfs. At the lower river discharges the main difference between the isotherm patterns in Figs. 9 and 11 is due to the different trajectories. In Fig. 11 the plumes are much wider when measured in feet, but not more than about ten percent wider when measured in units of normalized cumulative discharge $\Delta q_c/Q_R$. The significant difference is that in Fig. 9 the plume is confined to a narrow deep region of the channel where the velocities are high, but in Fig. 11 it tends to carry across the channel and blanket a wider, shallower region of the channel where the velocities are low. For Q_R = 10,000 cfs it was assumed that although the path of the plume is abruptly deflected

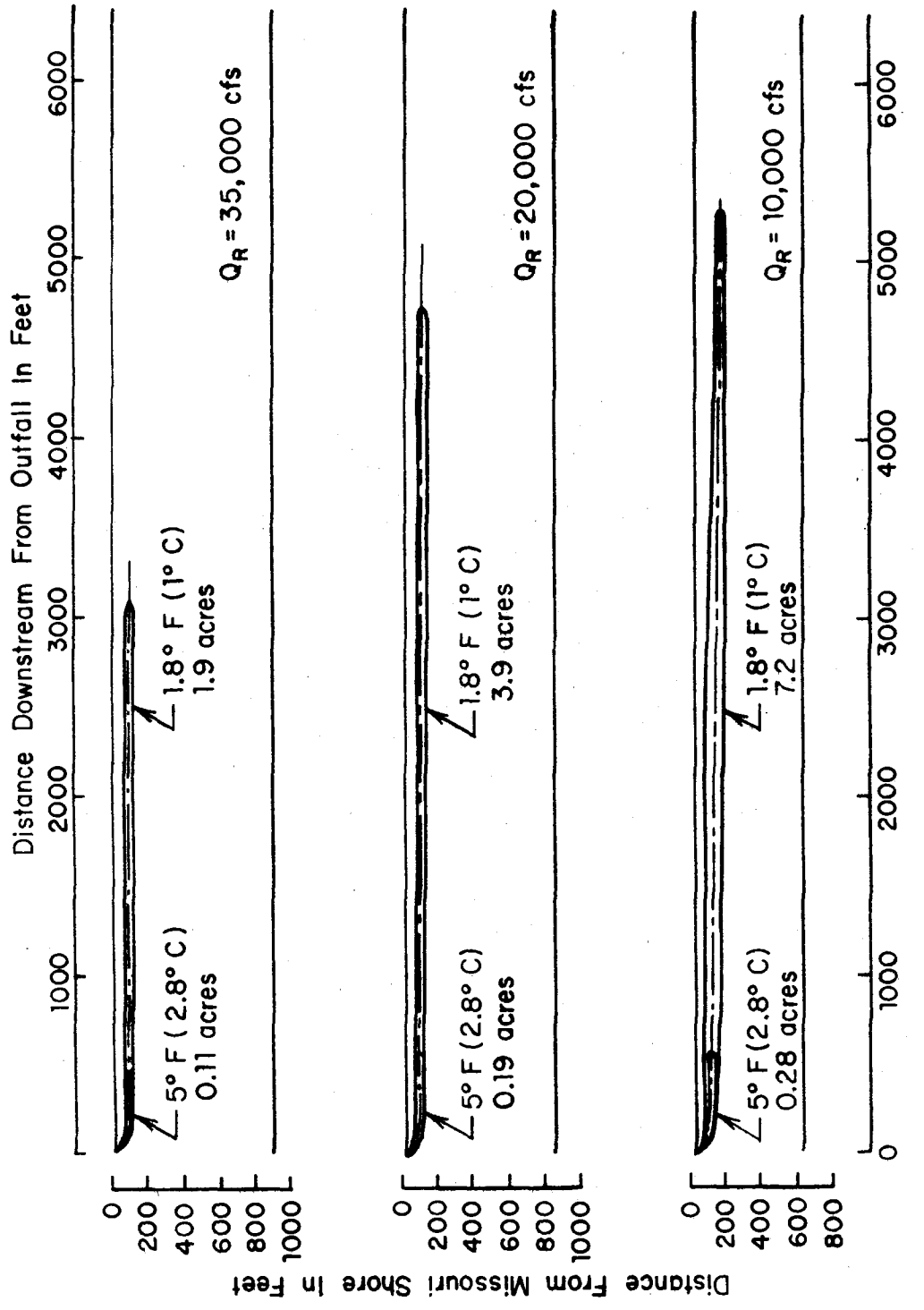

Figure 9. Predicted temperature-rise isotherms downstream from Iatan Station for 8-ft wide slot jet discharging at right angles to flow, 3-D trajectory.

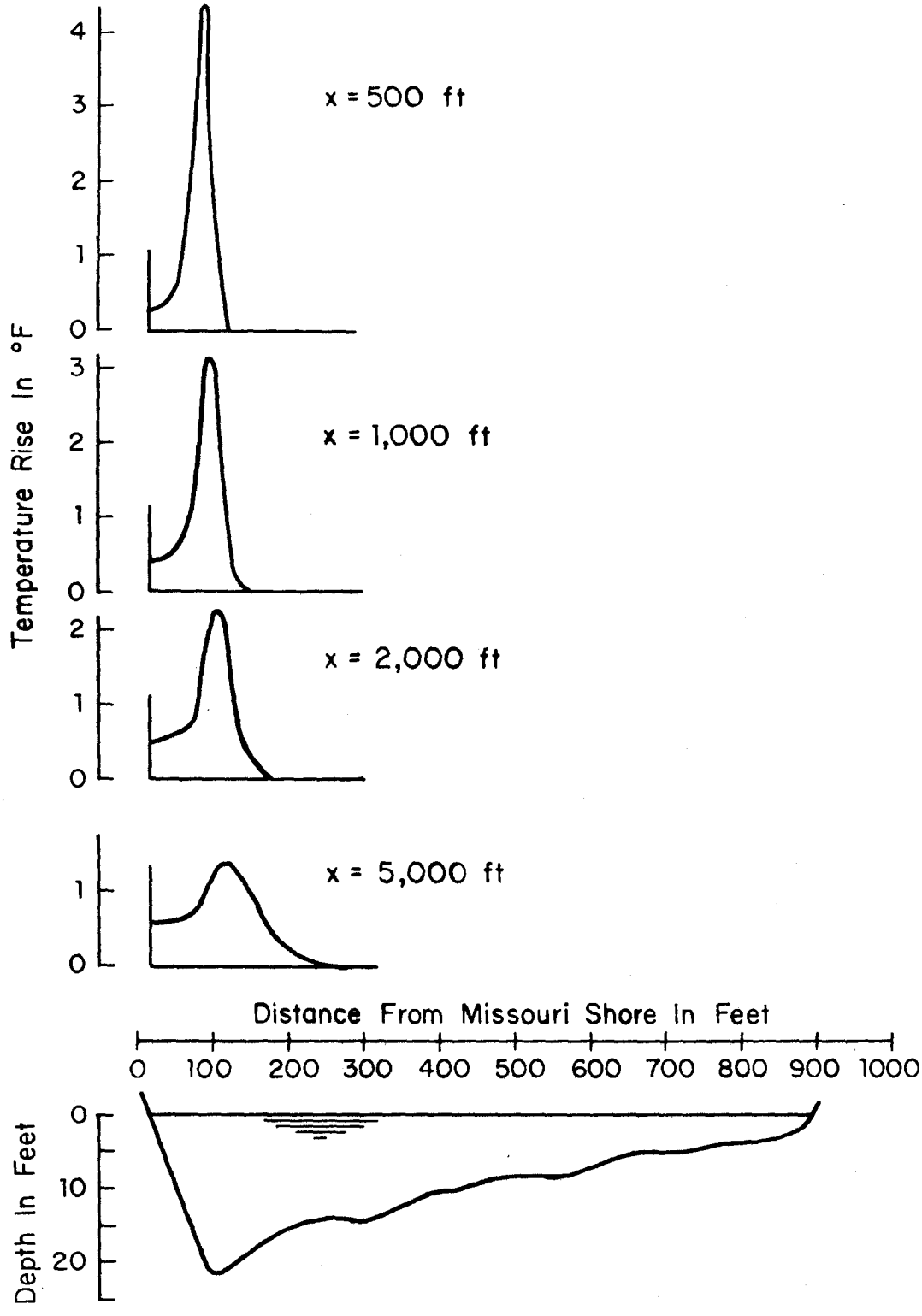

Figure 10a. Predicted transverse distribution of temperature rise; discharge at right angles, for Q_R = 35,000 cfs.

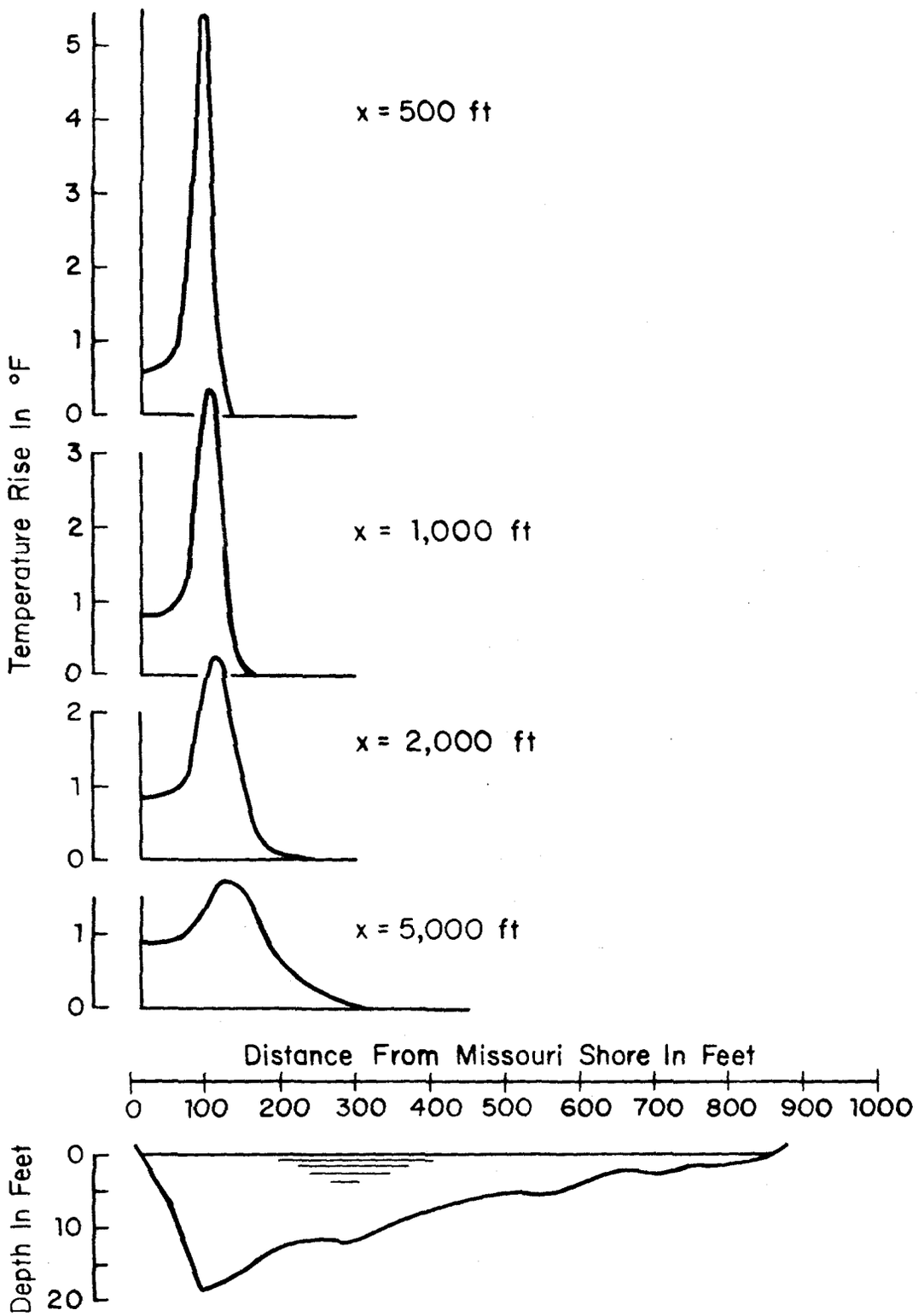

Figure 10b. Predicted transverse distribution of temperature rise; discharge at right angles, for Q_R = 20,000 cfs.

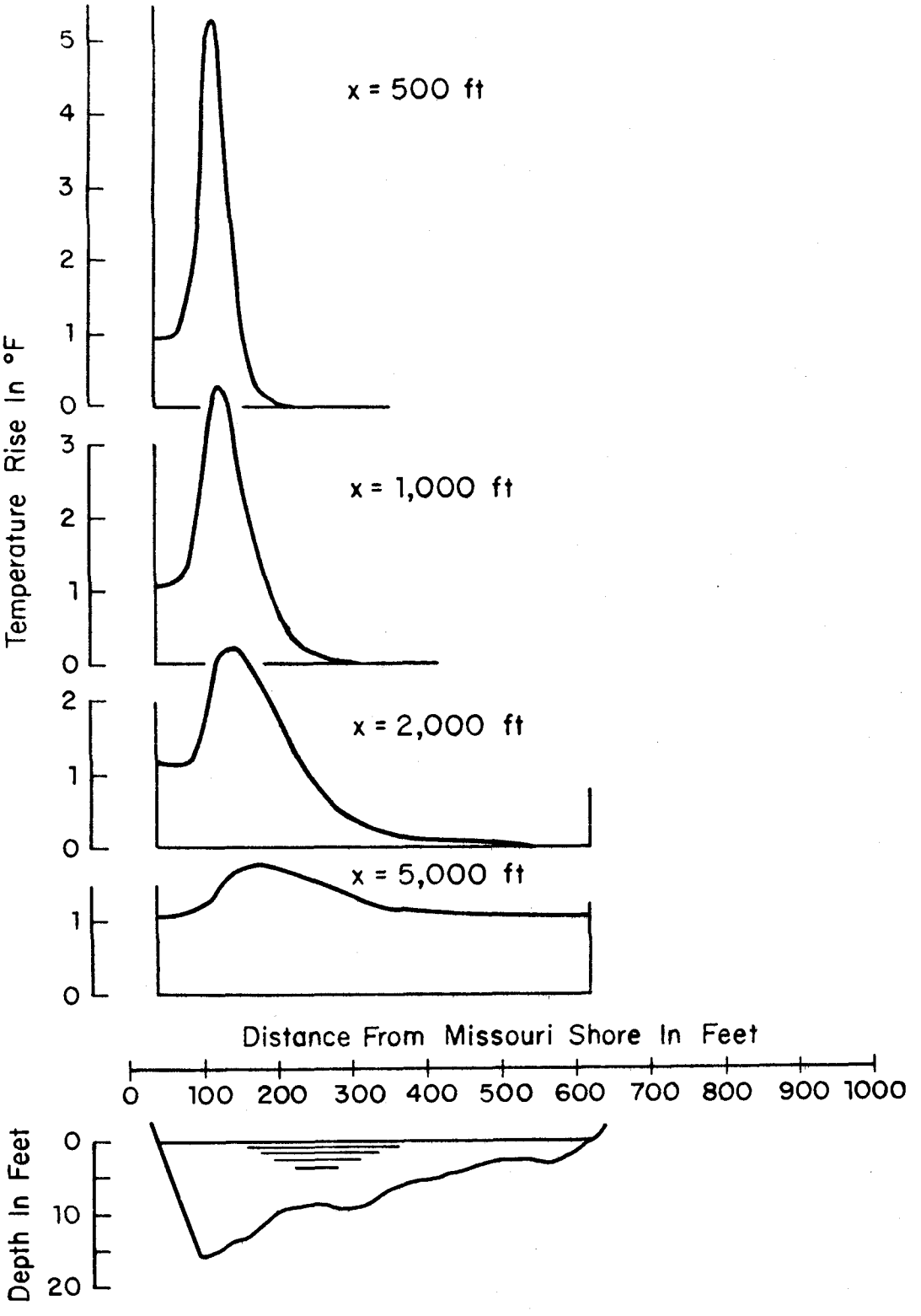

Figure 10c. Predicted transverse distribution of temperature rise; discharge at right angles, for Q_R = 10,000 cfs.

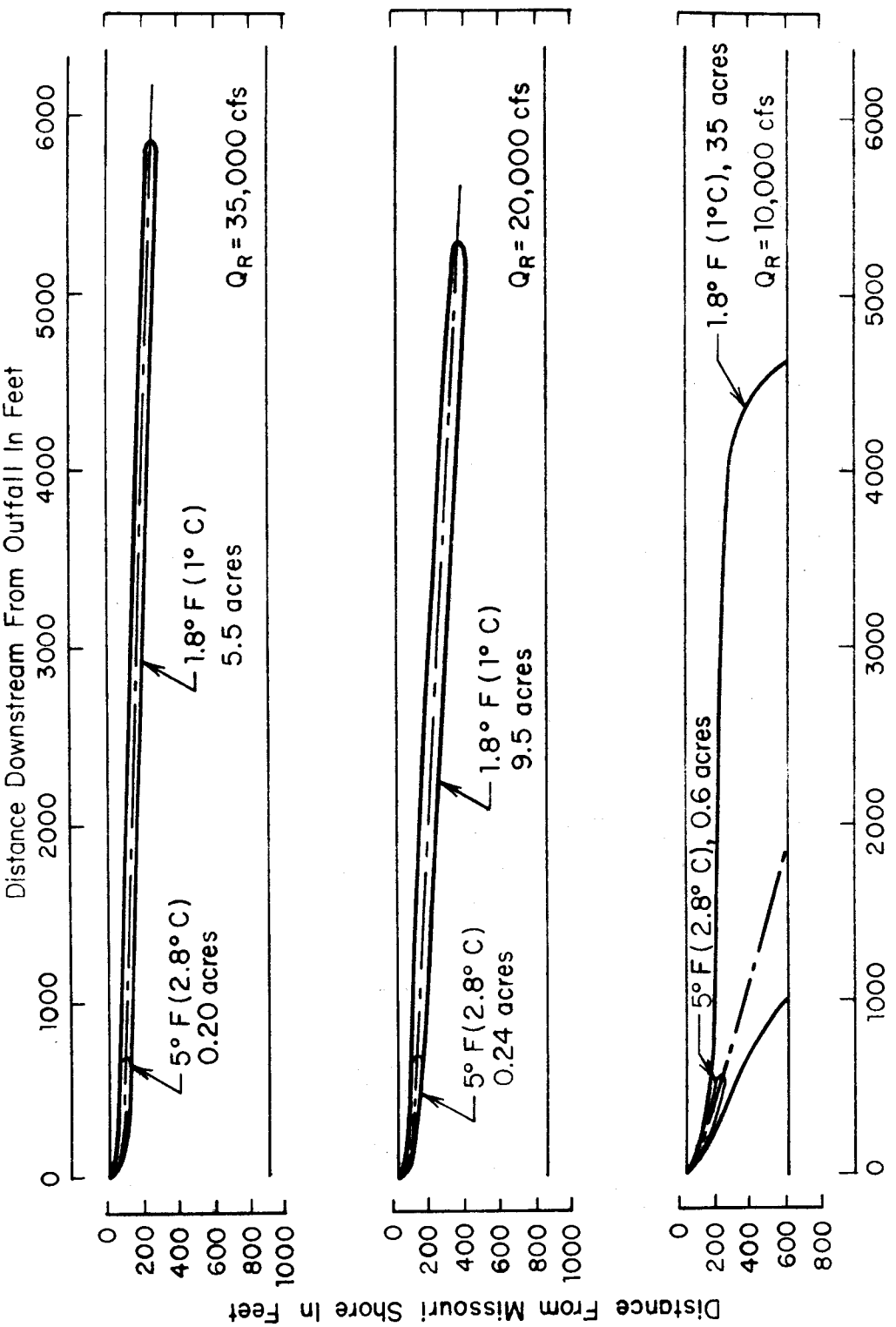

Figure 11. Predicted temperature-rise isotherms downstream from Tatan Station for 8-ft wide slot jet discharging at right angles to flow, 2-D trajectory.

in the downstream direction when it encounters the far shore, its width in terms of $\Delta q_c/Q_R$ is not affected. In the writer's estimation the isotherm pattern predicted in Fig. 9 is the more realistic one.

C. Results for Parallel Discharge. Fig. 12 shows sets of 10°F (5.6°C), 5°F (2.8°C) and 1.8°F (1°C) temperature-rise isotherms for the three river discharges. To show more detail in the near field region where temperature rises are higher, longitudinal distance is plotted on a logarithmic scale. The large variations in width of the regions enclosed by the 1.8°F isotherm for longitudinal distances greater than about 5,000 ft are due to shifts in the ambient flow pattern associated with the thalweg shifting back and forth across the channel. The logarithmic scale makes these variations appear much more abrupt than they really are. Transverse temperature-rise profiles together with cross-section profiles are shown in Figs. 13a - 13f for downstream distances of 500 ft, 2,100 ft (Section 1), 5,300 ft (Section 2), and 13,700 (Section 4). The large width of the plume at the downstream distance of 13,700 cfs is associated with the shift of the thalweg over to the Kansas side.

The temperature-rise isotherms in Fig. 12 and transverse distribution profiles in Figs. 13a - 13f were predicted using the modified diffusion model, Eqs. 26 - 31.

V. INTERPRETATION OF RESULTS

Comparison of the predicted results for the right-angle and parallel discharge cases indicates that the right-angle discharge is superior in almost every respect. Due to the slower mixing rate, the plumes for the parallel discharge case extend downstream much farther, particularly at the lower river discharges. There is no reduction in width with the increase in length. It just takes the plume longer to reach a given width. A particularly objectionable feature of the parallel-discharge results is the long distance over which high temperature rises persist along the Missouri shore. This may not be so bad for the first mile or so where there is a rock revetment along the shore and velocities and sediment concentrations tend to be high. However, for the next 1 1/2 miles there is a jetty field along the Missouri shore, which likely constitutes one of the more attractive fish habitats. The high temperature rises persist for long distances along the shore in the parallel

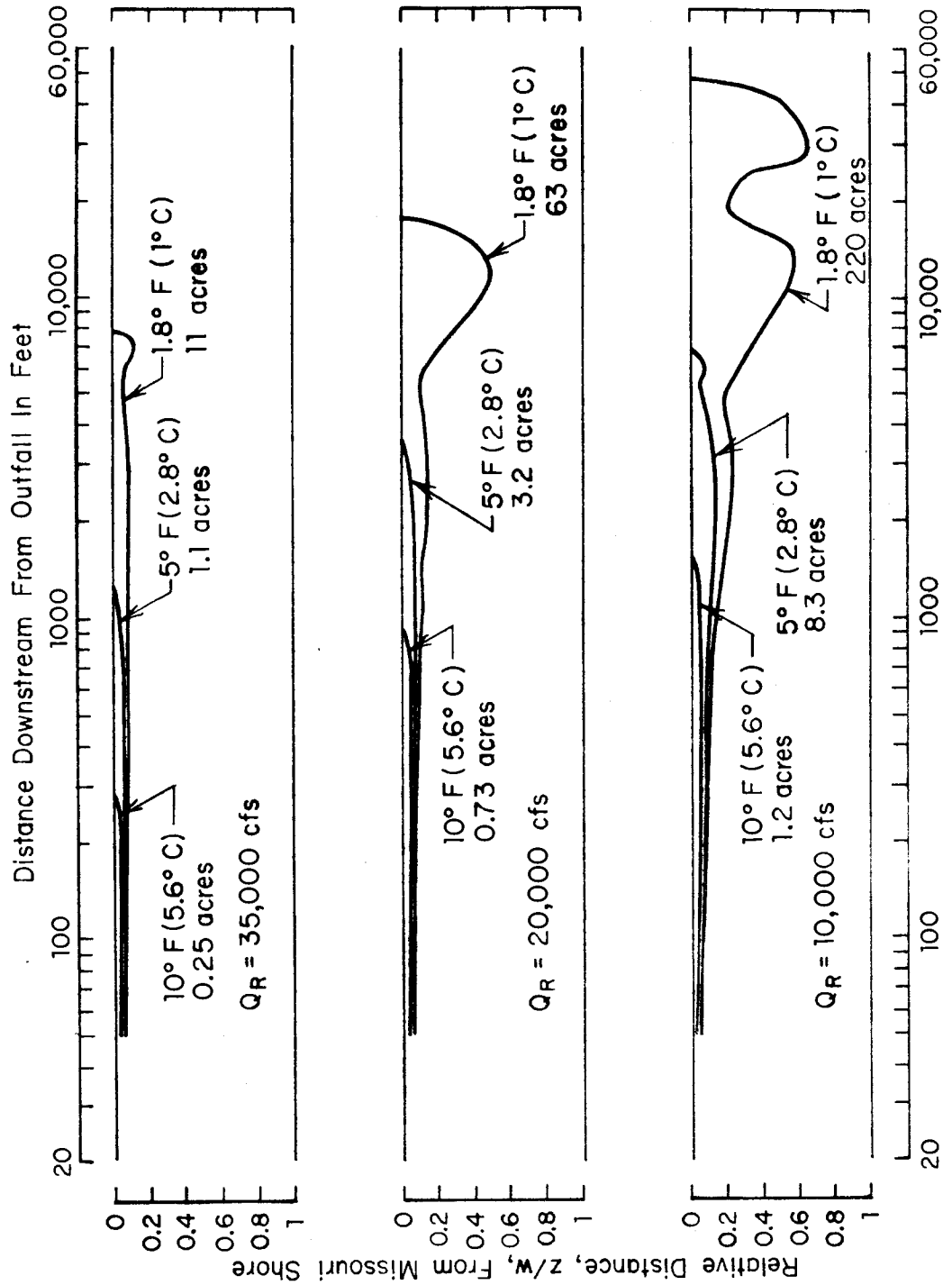

Figure 12. Predicted temperature-rise isotherms downstream from Iatan Station for 8-ft wide slot jet discharging parallel to flow.

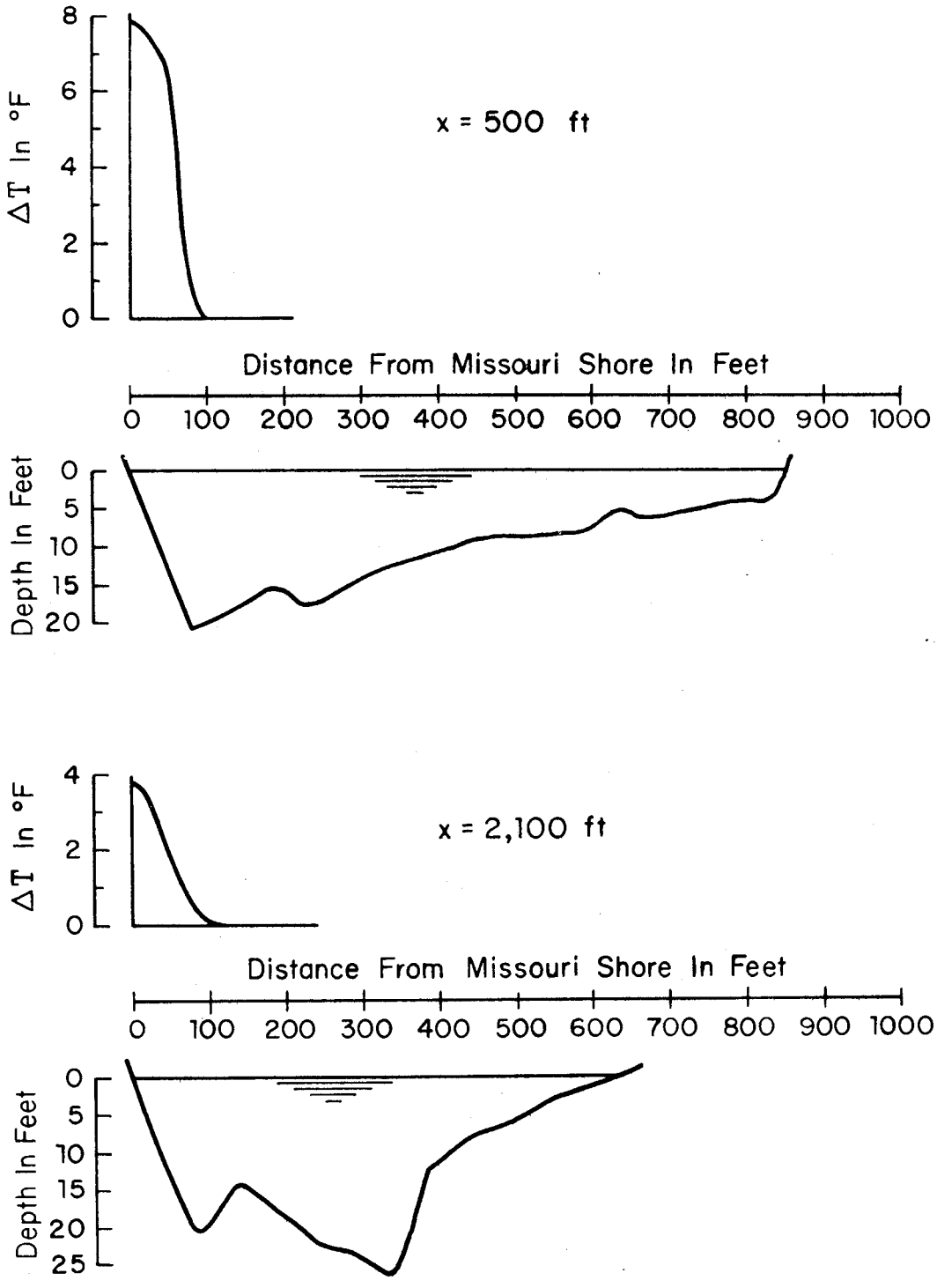

Figure 13a. Predicted transverse distribution of temperature rise; parallel discharge, for Q_R = 35,000 cfs, x = 500 and 2100 ft.

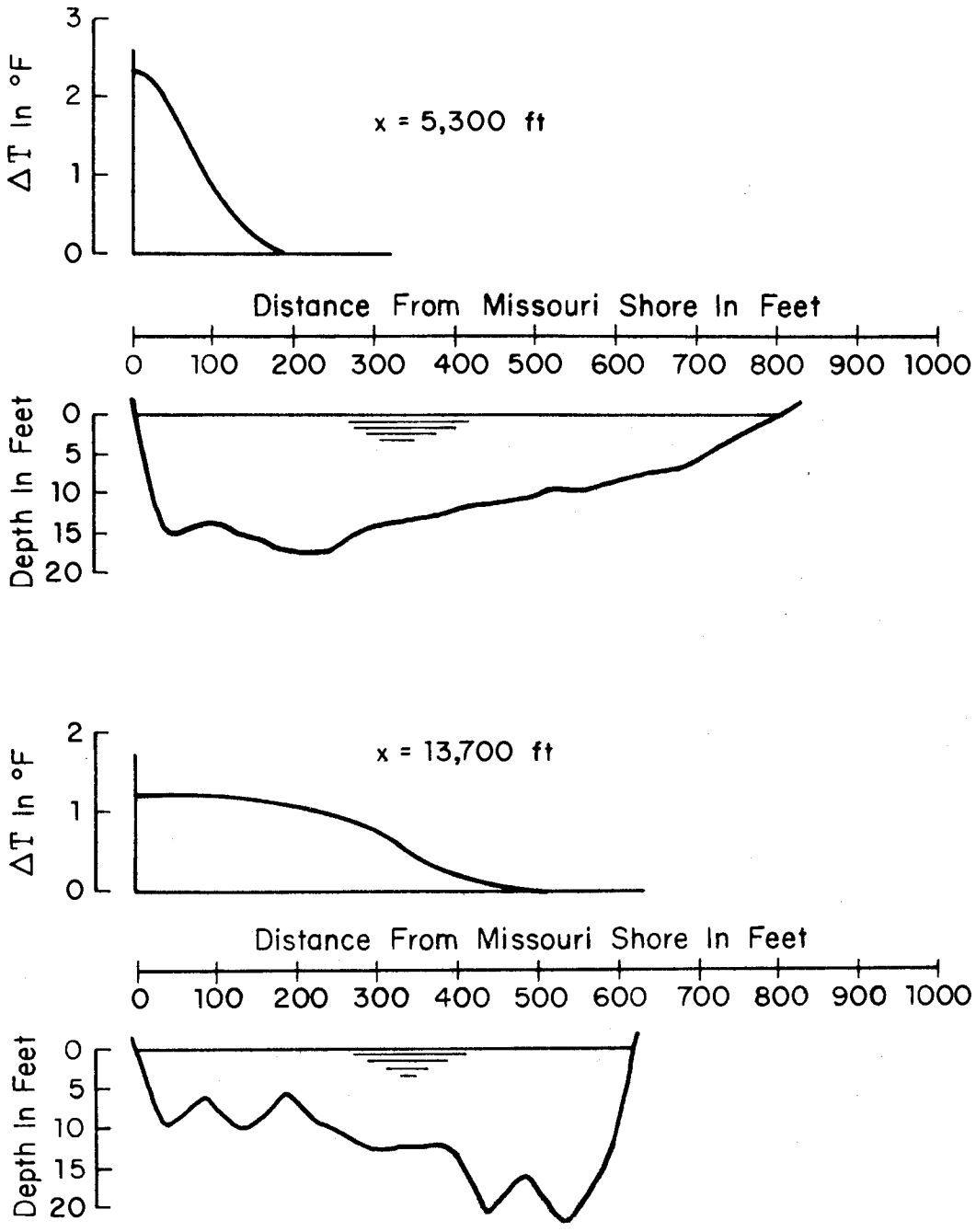

Figure 13b. Predicted transverse distribution of temperature rise; parallel discharge, for Q_R = 35,000 cfs, x = 5300 and 13,700 ft.